

DRY REFORMING OF METHANE USING COLD PLASMA REACTOR FOR
DIFFERENT DIELECTRIC MATERIALS AND MODIFIED MgAl_2O_4
CATALYSTS

ASIF HUSSAIN

A thesis submitted in fulfilment of the
requirements for the award of the degree of
Doctor of Philosophy

School of Chemical and Energy Engineering
Faculty of Engineering
Universiti Teknologi Malaysia

MARCH 2019

This thesis is dedicated to my beloved parents and teachers.

ACKNOWLEDGEMENT

In the name of Allah, the Lord of the worlds, the most Merciful, the most Compassionate; and prayers and peace be upon His messenger Mohammed (PBUH).

First and foremost, I must acknowledge my limitless thanks to my supervisor Prof. Ir. Dr. Nor Aishah Saidina Amin for her countless hours of reflecting, reading, encouraging and most of all patience through thick and thin of this study. I also present my thankfulness to the co-supervisor Dr. Muhammad Tahir for his guidance and support throughout the research period who remained more than generous with his expertise and precious time. I owe a deep debt of gratitude to University Teknologi Malaysia (UTM) and National University of Science and Technology (NUST) Pakistan for providing an opportunity to complete this work.

In addition, I am grateful to some researchers and academicians of the field, who worked hard with me from the beginning till the completion of the present research. Particularly, I highly appreciate the efforts expended by Dr. Faisal Mushtaq (BUIITEMS Quetta Pakistan), Dr. Muhammad Usman (NFC-IET Multan Pakistan) and Dr. Ramses Snoeckx (KAUST, Saudi Arabia). I would like to take this opportunity to say warm thanks to all my beloved friends, who have been so supportive along the way of doing my thesis.

Last but not least, I owe profound gratitude and wholehearted thankfulness to my family for their generous support they provided me throughout my entire life and particularly through the process of pursuing my doctoral endeavours. Because of their unconditional love and prayers, I have the chance to complete this thesis.

ABSTRACT

Dry reforming of methane (DRM) through dielectric barrier discharge (DBD) plasma is one of the promising techniques to convert greenhouse gases (GHGs) such as methane (CH_4) and carbon dioxide (CO_2) to syngas (H_2 , CO) and higher hydrocarbons. In this study, Ni-loaded $\text{La}_2\text{O}_3\text{-MgAl}_2\text{O}_4$ mix-matrix support lamella-structure catalyst is prepared using modified co-precipitation followed by hydrothermal and wetness incipient impregnation methods. The catalysts are characterised by X-ray diffraction, field emission scanning electron microscopy, high-resolution transmission electron microscopy, Brunauer-Emmett-Teller with N_2 , H_2 -temperature-programmed reduction and CO_2 -temperature-programmed desorption. The spent catalyst is characterised by scanning transmission electron microscopy, energy dispersive X-ray spectroscopy mapping, thermogravimetric analysis and dielectric properties. DRM activity test is carried-out to determine the influence of reactor configuration and dielectric materials on reactant processing and energy efficiency (EE). The reactor configurations include discharge gap, discharge length, volume discharge and catalyst volume are systematically studied to investigate the plasma-catalytic behaviour. The performance and regeneration of the prepared catalysts are tested in a catalytic-DBD reactor which depicts the CH_4 and CO_2 conversion 84 % and 85.5 %, respectively, while H_2 and CO selectivity are 51 % and 49.5 %, respectively ($\text{H}_2/\text{CO}=1.01$) with $\text{EE} = 0.13 \text{ mmol}\cdot\text{kJ}^{-1}$ for Ni/ $\text{La}_2\text{O}_3\text{-MgAl}_2\text{O}_4$ catalyst. The optimum process parameters were examined using multiple response surface methodology through a four-factors, five-level central composite design. The optimum values are feed flow rate = 18.8 mL min^{-1} , feed ratio = 1.05, input power = 125.6 W and catalyst loading = 0.6 g. Finally, from the macroscopic kinetics, the apparent activation energies are calculated as 32.6 kJ mol^{-1} and 35.2 kJ mol^{-1} for CH_4 and CO_2 , respectively. The calculated results fitted-well with the experimental results with ± 5 error. The catalytic-DBD reactor exhibits encouraging performance for DRM at larger a scale.

ABSTRAK

Pembaharuan kering metana (DRM) melalui plasma penyahcasan rintangan dielektrik (DBD) adalah salah satu teknik yang tampak menjanjikan untuk menukar gas rumah hijau (GHGs) seperti metana (CH_4) dan karbon dioksida (CO_2) kepada gas sintesis (H_2 , CO) serta hidrokarbon yang lebih tinggi. Dalam kajian ini, sokongan mangkin berstruktur lamela dibantu campuran-matrik La_2O_3 - MgAl_2O_4 bermuatan Ni telah disediakan dengan menggunakan kaedah ko-pemendakan terubahsuai diikuti dengan kaedah hidroterma dan kaedah pengisitepuan basah. Mangkin telah dicirikan oleh pembelauan sinar-X, mikroskopi elektron imbasan pancaran medan, mikroskopi elektron transmisi resolusi-tinggi, Brunauer-Emmett-Teller dengan nitrogen (BET), penurunan suhu berprogram dengan hidrogen dan penjerapan suhu teraturcara dengan CO_2 . Pasca-reaksi mangkin juga dicirikan oleh mikroskopi elektron transmisi imbasan, penyerakan tenaga sinar-X, analisis termogravimetri dan sifat dielektrik. Ujian aktiviti DRM telah dijalankan untuk menentukan pengaruh konfigurasi reaktor dan bahan dielektrik keatas pemprosesan dan kecekapan tenaga (EE) reaktan. Konfigurasi reaktor termasuk sela penyahcasan, panjang penyahcasan, isipadu penyahcasan dan isipadu mangkin telah dikaji secara sistematik untuk menyiasat kelakuan plasma bermangkin. Prestasi dan penjanaan semula mangkin yang disediakan telah diuji di dalam reaktor mangkin-DBD dimana menunjukkan penukaran CH_4 dan CO_2 masing-masing sebanyak 84% dan 85.5%, serta kememilihan H_2 dan CO masing-masing sebanyak 51% dan 49.5% ($\text{H}_2/\text{CO}=1.01$) dengan $\text{EE} = 0.13 \text{ mmol}\cdot\text{kJ}^{-1}$ bagi mangkin $\text{Ni}/\text{La}_2\text{O}_3$ - MgAl_2O_4 . Parameter proses optimum telah dikaji dengan menggunakan kaedah pelbagai respon permukaan melalui reka bentuk empat-faktor, lima-peringkat komposit pusat. Nilai optimum adalah jumlah kadar aliran masukan = 18.8 mL min^{-1} , nisbah masukan = 1.05, kuasa input = 125.6 W dan muatan mangkin = 0.6 g. Akhir sekali, daripada kajian kinetik makroskopik, tenaga pengaktifan yang dikira bagi CH_4 dan CO_2 masing-masing sebanyak 32.6 kJ mol^{-1} dan 35.2 kJ mol^{-1} . Keputusan yang dikira bersesuaian dengan keputusan eksperimen dengan ralat sebanyak ± 5 . Reaktor mangkin-DBD ini menunjukkan prestasi yang memberangsangkan untuk DRM pada skala besar.

TABLE OF CONTENTS

	TITLE	PAGE
	DECLARATION	ii
	DEDICATION	iii
	ACKNOWLEDGEMENT	iv
	ABSTRACT	v
	ABSTRAK	vi
	TABLE OF CONTENTS	vii
	LIST OF TABLES	xii
	LIST OF FIGURES	xiv
	LIST OF ABBREVIATIONS	xxiii
	LIST OF SYMBOLS	xxv
	LIST OF APPENDICES	xxvi
CHAPTER 1	INTRODUCTION	1
	1.1 Research Background	1
	1.2 Problem Statement	4
	1.3 Research Hypothesis	6
	1.4 Research Objectives	8
	1.5 Scope of the Study	8
	1.6 Significance of the Research	9
	1.7 Organization of the Study	10
CHAPTER 2	LITERATURE REVIEW	11
	2.1 Overview	11
	2.2 Non-Thermal Plasmas for DRM	15
	2.2.1 Features of Non-Thermal Plasma	15
	2.2.2 Basics and DRM Chemistry of DBD Plasma	17
	2.3 Challenges in DBD Plasma DRM	22

2.4	A Status and Recent Progress in Plasma-Catalysis	24
2.4.1	Plasma-Catalyst Interaction (Plasma-Catalysis)	24
2.4.2	Recent Development in NTP-DRM Catalysts	28
2.4.2.1	Transition and Noble Metal Catalysts	28
2.4.2.2	Perovskites and Spinel Structure Catalyst	38
2.5	Prospects in DBD Plasma Reactor Configuration	44
2.5.1	Basic Geometry of DBD Plasma	44
2.5.2	Different HV Electrode Morphologies	47
2.5.3	Discharge Volume or Discharge Zone	50
2.5.4	Dielectric Material (Reactor Tube)	54
2.5.5	Material Packing in DBD Reactor	59
2.6	Process Parameters and Kinetic Study	71
2.6.1	Process Parameters and Definitions	71
2.6.2	Kinetic Study of DRM in DBD Plasma	76
2.6.2.1	Global Kinetic Model	77
2.6.2.2	Power Law: A Macroscopic Kinetic Model for DBD	80
2.6.2.3	Semi-Empirical Power Law	82
2.7	Fluid Modelling of DBD Plasma	84
2.7.1	Zero-Dimensional (0D) Fluid Modelling	85
2.7.2	1D, 2D and 3D Fluid Modelling	87
2.8	Summary	90
CHAPTER 3 MATERIALS AND METHODS		93
3.1	Research Methodology	93
3.2	Materials	94
3.3	Catalyst Preparation	95
3.3.1	Preparation of Ni/ Al ₂ O ₃ - MgO	95
3.3.2	Preparation of MgAl ₂ O ₄	96
3.3.3	Preparation of La ₂ O ₃	97

3.3.4	Preparation of Ni/La ₂ O ₃ - MgAl ₂ O ₄	98
3.4	Material Characterization Methods	99
3.5	Experimental Setup and Reactor Configuration	101
3.5.1	Experimental Setup	101
3.5.2	Reactor Configuration	102
3.6	Calculations	105
3.7	Process Optimization and Kinetic Study	106
3.7.1	Process Optimization Study	106
3.7.2	Kinetic Study and Fluid Modelling	106
CHAPTER 4	MATERIAL CHARACTERIZATION	109
4.1	X-Ray Diffraction	109
4.2	FESEM and HRTEM Analysis	113
4.3	BET Surface Area	117
4.4	H ₂ -Temperature-Programmed Reduction	120
4.5	CO ₂ -Temperature-Programed Desorption	122
4.6	Dielectric Permittivity (Constant)	124
4.7	Summary	125
CHAPTER 5	REACTOR DESIGN AND MATERIAL PERFORMANCE	127
5.1	Dielectric Materials Performance in DBD DRM	127
5.1.1	Effect of GHSV	127
5.1.2	Effect of Feed Ratio	131
5.1.3	Effect of SIE	135
5.1.4	Carbon balance and Energy Efficiency (EE)	138
5.1.5	Characterization of Reactor Dielectric Materials	139
5.2	DBD Reactor Configuration	142
5.2.1	Effect of Discharge Gap	142
5.2.2	Effect of the Discharge Length and Volume	146
5.2.3	Effect of GHSV and V _{cat}	149

5.3	Plasma-Catalyst Activity	154
5.3.1	Catalyst Screening	154
5.3.2	Catalyst Stability	166
5.3.3	Characterization of Spent Catalyst	169
5.3.4	Regeneration of Catalyst	171
5.3.5	Reaction Mechanism	174
5.4	Summary	178
CHAPTER 6	PROCESS OPTIMIZATION USING RESPONSE SURFACE METHODOLOGY	181
6.1	Background	181
6.2	Design of Experiments (DoE)	182
6.3	Statistical Analysis Using RSM	186
6.3.1	Analysis of Regression Models	186
6.3.2	Effect of Processing Parameters on the Conversion of CH ₄ and CO ₂	192
6.3.3	Effect of Processing Parameters on H ₂ and CO Yield	195
6.3.4	Effect of Process Parameters on Energy Efficiency (EE)	198
6.4	Process Optimization and Model Validation	199
6.5	Summary	200s
CHAPTER 7	KINETIC STUDY AND FLUID MODELLING	203
7.1	Kinetic Model Description	203
7.2	Determination of Rate Constants	208
7.3	Parametric Effect on the Rate Constant and Conversion of Reactant Gases	209
7.3.1	Effect of Specific Input Energy (SIE)	209
7.3.2	Effect of Discharge Volume (V _D)	214
7.3.3	Effect of GHSV	218
7.4	Apparent Activation Energy	222
7.5	DBD Plasma Fluid Modelling	224
7.5.1	Background	226
7.5.2	Model description	226

7.5.3	Effect of Discharge Gap and Dielectric Constant Plasma Behaviour	226
7.6	Summary	237
CHAPTER 8	CONCLUSIONS AND RECOMMENDATIONS	239
8.1	Conclusions	239
8.2	Recommendations	242
REFERENCES		245
APPENDICES A-B		275 - 282

LIST OF TABLES

TABLE NO.	TITLE	PAGE
Table 2.1	Plasma-catalytic activity of the non-noble metal in DBD plasma DRM	32
Table 2.2	Plasma-catalytic activity of transition and noble metal catalysts in DBD plasma DRM	42
Table 2.3	Constituents on DBD plasma reactor configuration	45
Table 2.4	Effect of the DBD plasma reactor configuration on the conversion of feed gases	46
Table 3.1	Material list used in this work	94
Table 3.2	Physical properties of dielectric materials	95
Table 4.1	XRD analysis of the prepared fresh catalyst	111
Table 4.2	BET specific surface area and porous characteristics of prepared samples	120
Table 4.3	Analysis of reducibility of the prepared nanocatalysts	121
Table 4.4	CO ₂ uptake analysis of prepared samples at different temperatures	124
Table 5.1	Comparison of the effect of D _{gap} on the conversion of CH ₄ and CO ₂ in DBD plasma reactor.	144
Table 5.2	Effect of the V _D and GHSV on reactants conversion and EE in DBD plasma; feed ratio = 1, SIE =370 J ml ⁻¹ , D _{gap} = 3 mm, f=7.5 kHz.	149
Table 5.3	Experimental performance studies of DBD plasma DRM using 10%Ni/La ₂ O ₃ -MgAl ₂ O ₄ and comparison with the literature	165
Table 6.1	Design of experiments and independent variable ranges	183
Table 6.2	Full factorial CCD design matrix of independent variables along with experimental responses	184
Table 6.3	Summary of Analysis of Variance (ANOVA) for CCD catalytic DBD plasma DRM	188
Table 6.4	Model validation for catalytic DBD plasma DRM using 10% Ni/La ₂ O ₃ -MgAl ₂ O ₄ using optimized conditions	200
Table 7.1	Comparison of E _a in DRM over Ni/La ₂ O ₃ -MgAl ₂ O ₄ catalyst	225

Table 7.2	Possible reactions of electron impact with species of argon in homogenous DBD plasma reactor (Jonathan <i>et al.</i> , 2017)	229
-----------	--	-----

LIST OF FIGURES

FIGURE NO.	TITLE	PAGE
Figure 2.1	Dry reforming of methane and possible technological routes	12
Figure 2.2	DBD plasma parallel and cylindrical reactor configurations	18
Figure 2.3	Possible plasma-catalyst interface and various effects on the synergy of DBD plasma reactor system	28
Figure 2.4	SEM images of nickel manganese oxide (a) before DBD plasma reaction (b) after the DBD plasma reaction (Guo <i>et al.</i> , 2006)	38
Figure 2.5	TEM images of (a) Al ₂ O ₃ NRs 100 nm (b) Al ₂ O ₃ nanotubes 20 nm (c) Al ₂ O ₃ nano-lamella 10 nm (d) CeO ₂ NRs 100 nm (e) TiO ₂ NRs (f) Al ₂ O ₃ Nano lamella 20 nm (g) WO ₃ nano-lamella (Bell <i>et al.</i> , 2015; Chowdhury <i>et al.</i> , 2010; Kim <i>et al.</i> , 2003; Lee <i>et al.</i> , 2003; Tahir <i>et al.</i> , 2015; Wang <i>et al.</i> , 2014). Adapted with permission from (Kim <i>et al.</i> , 2003; Lee <i>et al.</i> , 2003; Wang <i>et al.</i> , 2014)	40
Figure 2.6	Typical geometry of dielectric barrier discharge (DBD) plasma reactor system	44
Figure 2.7	(a) Different reactor configurations based on the high voltage (HV) electrode morphology such as holes, porous and rough. DBD plasma DRM activity (a) conversions of CH ₄ (%) and (c) conversion of CO ₂ (%) in different feed flow rates and feed ratios (d) HV electrode coated by the catalyst. (b, c) Reproduced with permission from (Rico <i>et al.</i> , 2010b)	49
Figure 2.8	DBD plasma reactor with (a) single stage ionization D _L = 20 cm (b) multistage ionization D _L (5 cm) for each segment (Geometry and measurements are only for understanding). Reproduced with permission from (Wang <i>et al.</i> , 2009b)	53
Figure 2.9	CO ₂ conversion using different dielectric barriers ■ Ca _{0.7} Sr _{0.3} TiO ₃ added with 0.5 wt.% Li ₂ Si ₂ O ₅ ; ▲ Al ₂ O ₃ ; ● SiO ₂ (a) different voltage at constant frequency of 10 kHz (b) different input frequency at constant applied voltage. Reprinted with permission from (Li <i>et al.</i> , 2006)	56

Figure 2.10	Comparative instantaneous current profile and applied voltage at 13 kV, 2.5 % methane in argon with (a) quartz dielectrics, (b) alumina dielectrics (c) discharge power (P) (d) temperature of outer (ground) electrode to the reactor as function of applied voltage for a total flow-rate of 100 cm ³ min ⁻¹ and a methane concentration of 2.5 % in the feed for quartz and alumina. Reprinted with permission from (Kundu <i>et al.</i> , 2012)	57
Figure 2.11	2D Infrared Image temperature profile of the DBD reactor for four different dielectric materials and performance in different absorbed power. Reprinted with permission from (Ozkan <i>et al.</i> , 2016a)	58
Figure 2.12	(a) Mechanism of the electron diffusion, migration potential formation inside catalyst pores. Distribution of the electric potential for different pore sizes (b) 10 μm (c) 50 μm (d) 400 μm. Reprinted with permission from (Zhang <i>et al.</i> , 2016a)	61
Figure 2.13	Different reactor configurations based on packing material: (a) pre-packing catalytic plasma fixed bed DBD reactor (b) in situ fixed bed plasma DBD reactor (c) post packing fixed bed plasma DBD Reactor (d) fully packed bed plasma DBD reactor	64
Figure 2.14	Influence of the ferroelectric catalyst ((BFN=BaFe _{0.5} Nb _{0.5} O ₃) (BZT=BaZr _{0.75} Ti _{0.25} O ₃)) on the DBD plasma DRM activity in various applied voltages (a) conversion of CO ₂ (b) conversion of CH ₄ (c) CO selectivity (d) H ₂ selectivity (e) carbon balance (f) discharge power in different ferroelectric in various applied voltages. Reprinted with permission from (Chung <i>et al.</i> , 2014)	65
Figure 2.15	Methane conversion at equilibrium (thermal), DBD reactor (NTP) and packed bed DBD reactor in the D _{gap} using γ-Al ₂ O ₃ , Ni/γ-Al ₂ O ₃ and NiO/γ-Al ₂ O ₃ : (a) CH ₄ conversion (%) (b) H ₂ selectivity (%) Reactor temperature 300- 400 °C; total gas flow rate 170 ml min ⁻¹ ; discharge power 30 W; catalyst loading, 2 g; grains size 0.7–1.0 mm. Reproduced with permission from (Pietruszka and Heintze, 2004)	67
Figure 2.16	Influence of different catalyst packing on DRM activity in DBD plasma fixed bed reactor; (pressure, 1bar; wall temperature, 110 °C; CH ₄ /CO ₂ =1; feed flow rate, 50 mL min ⁻¹ ; discharge power, 110 W). Adapted with the permission from (Zhang <i>et al.</i> , 2015b)	69

Figure 2.17	Q-V Lissajous method to calculate average discharge power at applied voltage 10 kV and frequency 100 Hz. Reprinted with permission from (Zouaghi <i>et al.</i> , 2016). Copyright 2016 Elsevier B.V; (b) Temperature of catalytic DBD reactor as a function of input power. Reprinted with permission from (Zheng <i>et al.</i> , 2015a); (c) Effect of discharge power on the conversion of CH ₄ and CO ₂ (d) Selectivity of H ₂ and CO at flow rate 60 mL min ⁻¹ , CO ₂ /CH ₄ =1, D _L , 20 cm. Reprinted with permission from (Zhang <i>et al.</i> , 2010)	75
Figure 2.18	Rate of conversion over LaNiO ₃ catalytic DBD plasma using the global kinetic model: (a) CH ₄ ; and (b) CO ₂ . Reprinted with permission from Zheng <i>et al.</i> (2015c)	80
Figure 3.1	Flowchart of research methodology	93
Figure 3.2	Process flow diagram: preparation of MgAl ₂ O ₄	96
Figure 3.3	Process flow diagram: preparation of La ₂ O ₃ nano-particles	98
Figure 3.4	Process flow diagram: synthesis of Ni/La ₂ O ₃ -MgAl ₂ O ₄ catalyst	99
Figure 3.5	Schematic diagram of the DBD plasma reactor for dry reforming of methane (MFC) mass flow controller, (FCV) flow control valve	104
Figure 4.1	X-ray powder diffractogram (XRD) for prepared (a) 10 wt% Ni/ γ -Al ₂ O ₃ , 10 wt% Ni/MgO and 10 wt% Ni/ γ -Al ₂ O ₃ -MgO catalysts (b) MgAl ₂ O ₄ , La ₂ O ₃ , 10% Ni/MgAl ₂ O ₄ and 10 % Ni/La ₂ O ₃ -MgAl ₂ O ₄ samples	111
Figure 4.2	FESEM micrograph of prepared samples: (a-b) 10 wt% Ni/ γ -Al ₂ O ₃ -MgO with different magnifications; 1 μ m and 500 nm	113
Figure 4.3	FESEM micrograph of prepared samples: (a-b) MgAl ₂ O ₄ with different magnifications (a) 1 μ m (b) 200 nm (c-d) La ₂ O ₃ nano-particles with 1.0 μ m and 200 nm magnification (e-f) fresh 10% Ni/La ₂ O ₃ -MgAl ₂ O ₄ catalyst with 1.0 μ m 200 nm magnification	114
Figure 4.4	(a) EDX dot mapping of 10% Ni/La ₂ O ₃ -MgAl ₂ O ₄ (b) EDX elemental analysis 10% Ni/La ₂ O ₃ -MgAl ₂ O ₄ of using Point ID technique	115
Figure 4.5	HRTEM analysis of 10% Ni/La ₂ O ₃ -MgAl ₂ O ₄ (a) nano-lamella structure of MgAl ₂ O ₄ supported catalyst (b) high magnification TEM image for particle size analysis (c) HRTEM analysis of 10% Ni/La ₂ O ₃ -MgAl ₂ O ₄ for d-spacing (d) SAED pattern for 10% Ni/La ₂ O ₃ -MgAl ₂ O ₄	116
Figure 4.6	Nitrogen adsorption–desorption isotherms of prepared catalyst (a) 10% Ni/ γ -Al ₂ O ₃ , 10% Ni/MgO and 10% Ni/ γ -Al ₂ O ₃ -MgO (b) MgAl ₂ O ₄ and 10% Ni/La ₂ O ₃ -MgAl ₂ O ₄	118

Figure 4.7	B.J.H pore size distribution of fresh 10% Ni/ γ -Al ₂ O ₃ , 10% Ni/MgO, 10% Ni/ γ -Al ₂ O ₃ -MgO, MgAl ₂ O ₄ and 10% Ni/La ₂ O ₃ -MgAl ₂ O ₄	229
Figure 4.8	H ₂ -TPR profile for prepared samples (a) 10% Ni/ γ -Al ₂ O ₃ -MgO (b) 10% Ni/La ₂ O ₃ -MgAl ₂ O ₄	121
Figure 4.9	CO ₂ -TPD profile for prepared fresh samples (a) γ -Al ₂ O ₃ and 10% Ni/ γ -Al ₂ O ₃ -MgO (b) MgAl ₂ O ₄ and 10% Ni/La ₂ O ₃ -MgAl ₂ O ₄	123
Figure 4.10	Dielectric constant for prepared catalyst at 1.0 MHz frequency and temperature 25 °C	125
Figure 5.1	Effect of GHSV (h ⁻¹) (a) CH ₄ and CO ₂ conversion (b) H ₂ , CO and C ₂ H ₆ selectivity: D _{gap} = 3 mm, P = 140 W, feed ratio 1:1, D _L = 20 cm, f=7.5 kHz	128
Figure 5.2	Effect of GHSV (h ⁻¹) (a) H ₂ , CO and C ₂ H ₆ yield (b) SIE ; D _{gap} = 3 mm, P = 140 W, feed ratio 1:1, D _L = 20 cm, f=7.5 kHz	130
Figure 5.3	Effect of the feed ratio (a) CH ₄ and CO ₂ conversion (b) H ₂ , CO and C ₂ H ₆ selectivity: GHSV= 92 h ⁻¹ , SIE =370 J ml ⁻¹ , D _{gap} = 3 mm, D _L = 20 cm, f=7.5 kHz	133
Figure 5.4	Effect of the feed ratio (a) H ₂ , CO and C ₂ H ₆ yield (b) H ₂ /CO ratio; GHSV= 92 h ⁻¹ , SIE =370 J mL ⁻¹ , D _{gap} = 3 mm, D _L = 20 cm, f=7.5 kHz	134
Figure 5.5	Effect of specific input energy SIE (a) CH ₄ and CO ₂ conversion (b) H ₂ , CO and C ₂ H ₆ selectivity; GHSV= 92 h ⁻¹ , feed ratio = 1, D _{gap} = 3 mm, D _L = 20 cm, f=7.5 kHz	136
Figure 5.6	Effect of specific input energy SIE (a) H ₂ , CO and C ₂ H ₆ yield (d) input power vs average reactor temperature; GHSV= 92 h ⁻¹ , feed ratio = 1, D _{gap} = 3 mm, D _L = 20 cm, f =7.5 kHz	137
Figure 5.7	IR Imaging and temperature profile for both reactors (a) IR image for quartz reactor (b) IR image for alumina reactor: GHSV= 92 h ⁻¹ , feed ratio = 1, SIE =370 J ml ⁻¹ , D _{gap} = 3 mm, D _L = 20 cm, f=7.5 kHz	138
Figure 5.8	Performance analysis of DBD DRM for (a) carbon balance (b) EE; GHSV= 92 h ⁻¹ , feed ratio = 1, SIE =370 J ml ⁻¹ , D _{gap} = 3 mm, D _L = 20 cm, f=7.5 kHz	139
Figure 5.9	Raman spectra analysis for alumina reactor pre and post DRM in DBD plasma reactor	140
Figure 5.10	FE-SEM images (a-b) Alumina tube with different magnification (inside surface) pre-reaction in DBD plasma (d-e) formation of CNTs post-reaction in DBD plasma (c) EDX pre-reaction (f) EDX post-reaction	141

Figure 5.11	Effect of the D_{gap} on plasma-catalytic activity (a) CH_4 and CO_2 conversion (b) H_2 , CO and C_2H_6 selectivity (c) H_2 , CO and C_2H_6 yield: $\text{GHSV} = 92 \text{ h}^{-1}$, feed ratio = 1, $\text{SIE} = 370 \text{ J mL}^{-1}$, $D_{\text{gap}} = 3 \text{ mm}$, $D_L = 20 \text{ cm}$, $f = 7.5 \text{ kHz}$	145
Figure 5.12	(a) Schematic diagram of discharge length. Effect of the D_L and V_D on (b) CH_4 and CO_2 conversion: feed ratio = 1, $\text{SIE} = 370 \text{ J mL}^{-1}$, $D_{\text{gap}} = 3 \text{ mm}$, $f = 7.5 \text{ kHz}$	147
Figure 5.13	Effect of the D_L and V_D on (a) selectivity of H_2 , CO and C_2H_6 (b) yield of H_2 , CO and C_2H_6 ; feed ratio = 1, $\text{SIE} = 370 \text{ J mL}^{-1}$, $D_{\text{gap}} = 3 \text{ mm}$, $f = 7.5 \text{ kHz}$	148
Figure 5.14	Effect of GHSV (h^{-1}) corresponds to total feed flow rate ($10\text{-}50 \text{ mL min}^{-1}$) on the conversion and selectivity using Ni-AM; $\text{SIE} = 300 \text{ J mL}^{-1}$, catalyst loading = 0.5 g , $V_{\text{cat}} = 2.75 \text{ cm}^3$, $D_{\text{gap}} = 3 \text{ mm}$, $D_L = 20 \text{ cm}$) $V_D = 10.5 \text{ cm}^3$	151
Figure 5.15	Effect of GHSV (h^{-1}) correspond to the V_D variation at constant V_{cat} ; feed flow rate ($=20 \text{ mL min}^{-1}$) $\text{SIE} = 300 \text{ J mL}^{-1}$, feed ratio = 1, $D_{\text{gap}} = 3 \text{ mm}$, catalyst loading (10% Ni/ $\gamma\text{-Al}_2\text{O}_3\text{-MgO}$) = 0.5 g	153
Figure 5.16	Effect of GHSV (h^{-1}) correspond to V_{cat} and V_D variation in 10% Ni/ $\gamma\text{-Al}_2\text{O}_3\text{-MgO}$ (a) 0.5 g (b) 1.0 g (c) 2 g ; feed flow rate = 20 mL min^{-1} , feed ratio = 1, $\text{SIE} = 300 \text{ J mL}^{-1}$, $D_{\text{gap}} = 3 \text{ mm}$	153
Figure 5.17	Effect of Ni loading on the plasma-catalytic activity of Ni/ $\gamma\text{-Al}_2\text{O}_3\text{-MgO}$ (a) conversion of CH_4 and CO_2 (b) selectivity of H_2 , CO and C_2H_6 ; $\text{GHSV} = 364 \text{ h}^{-1}$, feed ratio = 1, $\text{SIE} = 300 \text{ J mL}^{-1}$, $D_{\text{gap}} = 3 \text{ mm}$, $D_L = 20 \text{ cm}$, $f = 7.5 \text{ kHz}$, catalyst loading = 0.5 g and $V_D = 9.75 \text{ cm}^3$	156
Figure 5.18	Plasma-catalytic performance evaluation of prepared samples on (a) CH_4 conversion (b) CO_2 conversion; $\text{GHSV} = 364 \text{ h}^{-1}$, feed ratio = 1, $\text{SIE} = 300 \text{ J mL}^{-1}$, $D_{\text{gap}} = 3 \text{ mm}$, $D_L = 20 \text{ cm}$, $f = 7.5 \text{ kHz}$, catalyst loading = 0.5 g and $V_D = 9.75 \text{ cm}^3$	158
Figure 5.19	Plasma-catalytic performance evaluation of prepared samples on (a) H_2 selectivity (b) CO selectivity; $\text{GHSV} = 364 \text{ h}^{-1}$, feed ratio = 1, $\text{SIE} = 300 \text{ J mL}^{-1}$, $D_{\text{gap}} = 3 \text{ mm}$, $D_L = 20 \text{ cm}$, $f = 7.5 \text{ kHz}$, catalyst loading = 0.5 g and $V_D = 9.75 \text{ cm}^3$	160
Figure 5.20	Plasma-catalytic performance evaluation of prepared samples on (a) C_2H_6 selectivity (b) H_2/CO ratio; $\text{GHSV} = 364 \text{ h}^{-1}$, feed ratio = 1, $\text{SIE} = 300 \text{ J mL}^{-1}$, $D_{\text{gap}} = 3 \text{ mm}$, $D_L = 20 \text{ cm}$, $f = 7.5 \text{ kHz}$, catalyst loading = 0.5 g and $V_D = 9.75 \text{ cm}^3$	162

Figure 5.21	Plasma-catalytic performance evaluation of prepared samples on (a) carbon balance C_B (%) (b) EE mmol kJ^{-1} ; GHSV= 364 h^{-1} , feed ratio = 1, SIE = 300 J mL^{-1} , $D_{\text{gap}} = 3 \text{ mm}$, $D_L = 20 \text{ cm}$, $f = 7.5 \text{ kHz}$, catalyst loading = 0.5 g and $V_D = 9.75 \text{ cm}^3$	163
Figure 5.22	Effect of time on stream (TOS) (h): (a) conversion of CH_4 and CO_2 H_2 and CO selectivity (b) H_2 and CO yield, C_2H_4 selectivity and H_2/CO ratio (c) energy efficiency (EE) mmol kJ^{-1} (d) carbon balance C_B (%); GHSV 364 h^{-1} , SIE = 300 J mL^{-1} , catalyst loading = 0.5 g , $D_{\text{gap}} = 3 \text{ mm}$, $D_L = 20 \text{ cm}$, $V_D = 9.75 \text{ cm}^3$	168
Figure 5.23	(a) XRD pattern of the spent catalyst $\text{Ni/La}_2\text{O}_3\text{-MgAl}_2\text{O}_4$ (b) TGA profile for spent catalyst after 15 h operation time (c-d) FESEM of spent catalyst with different magnification	170
Figure 5.24	(a) EDX dot-mapping for the spent catalyst (b) EDX dot ID elemental analysis for spent catalyst	171
Figure 5.25	Plasma-catalytic activity of the regenerated catalyst 10% $\text{Ni/La}_2\text{O}_3\text{-MgAl}_2\text{O}_4$ over 15 h TOS (a) CH_4 Conversion (b) CO_2 conversion (c) EE mmol kJ^{-1} (d) H_2/CO ratio; GHSV = 364 h^{-1} , SIE = 300 J mL^{-1} , catalyst loading = 0.5 g , $D_{\text{gap}} = 3 \text{ mm}$, $D_L = 20 \text{ cm}$, $V_D = 9.75 \text{ cm}^3$	172
Figure 5.26	Plasma catalytic activity of the regenerated catalyst 10% $\text{Ni/La}_2\text{O}_3\text{-MgAl}_2\text{O}_4$ (a) H_2 selectivity (b) CO selectivity (c) H_2 yield (d) CO yield; GHSV = 364 h^{-1} , SIE = 300 J mL^{-1} , catalyst loading = 0.5 g , $D_{\text{gap}} = 3 \text{ mm}$, $D_L = 20 \text{ cm}$, $V_D = 9.75 \text{ cm}^3$	174
Figure 5.27	(a) Catalyst regeneration mechanism over 10 % $\text{Ni/La}_2\text{O}_3\text{-MgAl}_2\text{O}_4$ in DBD plasma (b) reaction mechanism over 10% $\text{Ni/La}_2\text{O}_3\text{-MgAl}_2\text{O}_4$	177
Figure 6.1	Pareto-chart and parity-plot for developed regression models for dependent variables: (a) CH_4 conversion (y_1) (b) CO_2 conversion (y_2)	189
Figure 6.2	Pareto-chart and parity-plot for developed regression models for dependent variables: (a) H_2 yield (y_3) (b) CO yield (y_4)	191
Figure 6.3	Pareto-chart and parity-plot for developed regression models for energy efficiency (EE, mmol kJ^{-1}) y_1	192
Figure 6.4	Three dimensional responses and contour plot; effect of the process parameters of the conversion of (y_{CH_4}) CH_4 : (a) flow rate and input power; (feed ratio = 1, catalyst loading = 0.5 g) (b) flow rate and catalyst loading; ($P = 100 \text{ W}$, feed ratio = 1) (c) flow rate and feed ratio ($P = 100 \text{ W}$, catalyst loading = 0.5 g) (d) input power and catalyst loading (total flow rate = 20 mL min^{-1} , feed ratio = 1)	194

Figure 6.5	Three dimensional responses and contour plot; effect of the process parameters on conversion of (y_{CO_2}) CO_2 : (a) input power and flow rate; (feed ratio =1, catalyst loading = 0.5 g) (b) flow rate and catalyst loading; (P = 100 W, feed ratio = 1) (c) flow rate and feed ratio; (P =100 W, Cat loading = 0.5 g) (d) input power and catalyst loading; (flow rate =20 ml min ⁻¹ , feed ratio =1)	195
Figure 6.6	Three dimensional responses and contour plot; effect of process parameters on H ₂ yield (y_{H_2}): (a) feed ratio and feed flow rate; (P =100 W, feed ratio =1) (b) feed flow rate and input power (feed ratio =1, catalyst loading = 0.5 g) (c) feed flow rate and catalyst loading (P = 100 W, feed ratio = 1) (d) feed ratio and catalyst loading (feed flow rate = 20 ml min ⁻¹ , P =100 W)	196
Figure 6.7	Three dimensional responses and contour plot; effect of process parameters on CO yield (y_{CO}): (a) feed ratio and feed flow rate (P =100 W, catalyst loading = 0.5 g) (b) feed flow rate and input power (feed ratio =1, catalyst loading = 0.5 g) (c) feed flow rate and catalyst loading (P = 100 W, feed ratio =1) (d) input power and catalyst loading (feed flow rate = 20 ml min ⁻¹ , feed ratio = 1)	197
Figure 6.8	Effect of the process parameters on EE (kJ mol ⁻¹) (y_{EE}) demonstrated in three dimensional surface responses and contour plots : (a) feed ratio and feed flow rate (P = 100 W, catalyst loading = 0.5 g) (b) flow rate and catalyst loading; (P = 100 W, feed ratio = 1) (c) feed flow rate and input power (feed ratio = 1, catalyst loading = 0.5 g) (d) feed ratio and catalyst loading (P = 100 W, feed flow rate = 20 ml min ⁻¹)	199
Figure 7.1	Schematic diagram and boundary condition of catalytic-DBD plasma reactor for DRM process	203
Figure 7.2	Effect of the specific input energy (SIE) on the rate constants k_{CH_4} and k_{CO_2} ; feed flow rate = 20 ml min ⁻¹ , feed ratio =1, catalyst loading = 0.5 g, applied frequency = 7.8 kHz	211
Figure 7.3	Comparison between experimental and calculated results. Effect of the SIE on reactant conversion (a) CH ₄ conversion (b) CO ₂ conversion; feed flow rate = 20 ml min ⁻¹ , feed ratio =1, catalyst loading = 0.5 g, frequency =7.8 kHz	212
Figure 7.4	Effect of the SIE on reactant conversion (a) products yield (b) H ₂ /CO ratio, C_B and EE; P = 100 W, feed flow rate =20 ml min ⁻¹ , feed ratio =1, catalyst loading = 0.5 g, frequency = 7.8 kHz	213

Figure 7.5	Effect of the discharge volume V_D (cm^3) on the rate constants k_{CH_4} and k_{CO_2} ; feed flow rate = 20 ml min^{-1} , SIE = 300 J ml^{-1} , catalyst loading = 0.5 g , feed ratio =1, frequency = 7.8 kHz	214
Figure 7.6	Comparison between experimental and calculated results. Effect of the V_D on reactant conversion (a) CH_4 conversion (b) CO_2 conversion; feed flow rate = 20 ml min^{-1} , SIE = 300 J ml^{-1} , feed ratio =1, catalyst loading = 0.5 g , frequency $7.8 = \text{kHz}$	216
Figure 7.7	Effect of the V_D on (a) CH_4 conversion (b) CO_2 conversion; feed flow rate 20 ml min^{-1} , SIE = 300 J ml^{-1} , feed ratio =1, catalyst loading = 0.5 g , frequency = 7.8 kHz	217
Figure 7.8	Effect of the GHSV (h^{-1}) on the rate constants k_{CH_4} and k_{CO_2} ; $P = 300 \text{ W}$, feed ratio=1, catalyst loading = 0.5 g , frequency = 7.8 kHz	219
Figure 7.9	Comparison between experimental and calculated results. Effect of the GHSV (h^{-1}) on reactant conversion (a) CH_4 conversion (b) CO_2 conversion; $P = 100 \text{ W}$, feed ratio =1, catalyst loading = 0.5 g , frequency = 7.8 kHz	210
Figure 7.10	Effect of the GHSV (h^{-1}) on (a) products yield (b) H_2/CO ratio, C_B and EE; $P = 100 \text{ W}$, feed ratio =1, catalyst loading = 0.5 g , frequency = 7.8 kHz	221
Figure 7.11	Arrhenius plot for Ni/La ₂ O ₃ -MgAl ₂ O ₄ loaded hybrid-DBD plasma DRM (a) CH_4 (b) CO_2 in various reactor temperatures	224
Figure 7.12	One-Dimensional geometry used in the simulation for spatial-temporal behaviour of Ar-based DBD reactor	227
Figure 7.13	Surface plot: Effect of the dielectric permittivity (ϵ_r) on mass fraction of excited argon in various discharge gap (10^{-4} mm) in Ar-based DBD plasma (a) $\epsilon_r = 10$ (b) $\epsilon_r = 20$ (c) $\epsilon_r = 50$ (d) $\epsilon_r = 100$	230
Figure 7.14	Surface plot: Effect of the dielectric constant (ϵ_r) on electric field (Vm^{-1}) in various discharge gap length (1-6 mm) in Ar-based DBD plasma (a) $\epsilon_r = 10$ (b) $\epsilon_r = 20$ (c) $\epsilon_r = 50$ (d) $\epsilon_r = 100$	231
Figure 7.15	Effect of the dielectric permittivity (ϵ_r) on mean electron energy (eV) (Vm^{-1}) in various discharge gap length (1-6 mm) in Ar-based DBD plasma (a) $\epsilon_r = 10$ (b) $\epsilon_r = 20$ (c) $\epsilon_r = 50$ (d) $\epsilon_r = 100$	231
Figure 7.16	Line graph for various segments: Effect of the dielectric permittivity (ϵ_r) on electron temperature profile (eV) ($8.617 \times 10^{-5} = 1\text{K}$) in various discharge gap length (1-6 mm) in Ar-based DBD plasma (a) $\epsilon_r = 10$ (b) $\epsilon_r = 20$ (c) $\epsilon_r = 50$ (d) $\epsilon_r = 100$	233

Figure 7.17	Surface plot: Effect of the dielectric permittivity (ϵ_r) on Ar ion density in various discharge gap in Ar-based DBD plasma (a) $\epsilon_r = 10$ (b) $\epsilon_r = 20$ (c) $\epsilon_r = 50$ (d) $\epsilon_r = 100$	234
Figure 7.18	Line graph for various segment points: Effect of the dielectric permittivity (ϵ_r) on electron density in various discharge gap in Ar-based DBD plasma (a) $\epsilon_r = 10$ (b) $\epsilon_r = 20$ (c) $\epsilon_r = 50$ (d) $\epsilon_r = 100$	235
Figure 7.19	Surface plot: Effect of the dielectric permittivity (ϵ_r) on electron density in various discharge gap in Ar-based DBD plasma (a) $\epsilon_r = 10$ (b) $\epsilon_r = 20$ (c) $\epsilon_r = 50$ (d) $\epsilon_r = 100$	236

LIST OF ABBREVIATIONS

BET	-	Brunauer-Emmet-Teller
C	-	Capacitance
DBD	-	Dielectric Barrier Discharge
D_e	-	Diffusion coefficient
D_{gap}	-	Discharge gap
D_L	-	Discharge Length
DRM	-	Dry Reforming of Methane
E	-	Electric field
E_a	-	Activation Energy
EDX	-	Energy Dispersion X-ray
EE	-	Energy Efficiency
f	-	Frequency
FID	-	Flame Ionization Detector
GC	-	Gas Chromatograph
GHG	-	Greenhouse Gas
GHSV	-	Gas Hourly Space Velocity
I	-	Current
PBR	-	Packed Bed Reactor
P_X	-	Partial Pressure
R	-	Gas constant
r	-	Radius
R_T	-	Residence Time
SIE	-	Specific Input Energy
S_X	-	Selectivity
T	-	Temperature
TCD	-	Thermal Conductivity Detector
TEM	-	Transmission Electron Microscopy
TOS	-	Time on Stream
TPD	-	Temperature Programmed Oxidation

TPR	-	Temperature Programmed Reduction
V_D	-	Discharge Volume
V_e	-	Volume of electrode
V_t	-	Volume of tube
X_n	-	Conversion
XRD	-	X-Ray Diffraction
Y	-	Yield

LIST OF SYMBOLS

π	-	Pi
μ	-	Micro
ϵ	-	Permittivity/Dielectric constant
μ_e	-	Electron mobility
ω	-	Empirical coefficient
γ	-	Gamma
n_x	-	Number of moles of x specie
τ	-	Residence time
EE	-	Energy Efficiency
FID	-	Flame Ionization Detector
GC	-	Gas Chromatograph
GHG	-	Greenhouse Gas
GHSV	-	Gas Hourly Space Velocity
PBR	-	Packed Bed Reactor
P_x	-	Partial Pressure
R	-	Gas constant

LIST OF APPENDICES

APPENDIX	TITLE	PAGE
Appendix A	List of Publications	275
Appendix B	Calculation and Plasma-Catalytic Activities And Plasma Characteristics	277

CHAPTER 1

INTRODUCTION

1.1 Research Background

The escalation in energy demand and depletion of fossil fuels are two major challenges for sustainable development. The energy demand and global warming are alarming entities must be addressed on time; otherwise, the world will be facing huge energy crises and serious global warming issues. The global warming caused due to the emissions of Greenhouse Gases (GHGs) which effects climate change, disturbing human and aquatic life (Kennedy *et al.*, 2009). Fossil fuels utilization is one of the major causes of emission of GHGs. The main contributors of GHGs are CH₄ and CO₂, with 16% and 76% share respectively (Lane, 2016; Parker *et al.*, 2018). To address these two distinct threats, different approaches have been made to produce clean energy via utilization of GHGs (Covert *et al.*, 2016; Liu *et al.*, 2003). Over the last decade, researchers are taking key attention to reduce GHG emissions by utilizing them to produce energy for sustainable development. The serious concerns about energy crises have been predicted by researchers by 2035 (Duan *et al.*, 2015b; OECD, 2015). Energy is considered one of the core concerns in developing regions like African countries and Asian countries. The utilization of GHGs to produce energy carriers is yet to commercialized due to serious limitations (Covert *et al.*, 2016; Lane, 2016).

Currently the scientific community is utilizing the GHGs through different technologies to minimize the CO₂ and CH₄ concentration from atmosphere and produce energy, especially reforming technologies i.e., CO₂ or dry reforming of methane (DRM), partial oxidation of methane (POM) (Song *et al.*, 2017), oxidative coupling of methane (OCM) and photocatalytic conversion of methane and CO₂ (Liu

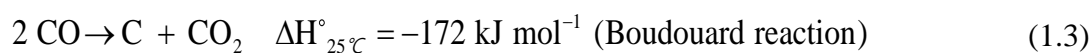
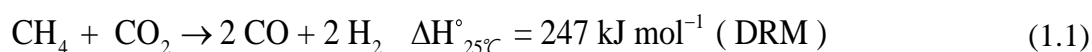
et al., 2003; Tahir and Amin, 2013). One of the promising technique, which is getting much attention from the last decade is DRM (Equation 1.1) for the production of valuable fuels like syngas (H_2 , CO) and other HCs (Wang *et al.*, 2018b; Zhang and Verykios, 1994). DRM can be considered via three major approaches (i) thermal DRM and (ii) photo-catalytic DRM (iii) plasma DRM (Bromberg *et al.*, 1998; Eliasson *et al.*, 2000; Jean Marie and Iulian, 2001; Jiang *et al.*, 2002). Plasma DRM is again sub-categorized into two major kinds (i) Thermal plasma (ii) Non-Thermal Plasma (NTP). The plasma is an ionized gas that can be generated by different methods including electric discharges depending upon their energy level, electron temperature and ionic density (Bromberg *et al.*, 1998; Indarto *et al.*, 2008; Neyts *et al.*, 2015; Whitehead, 2016).

In thermal plasmas, the temperature of gas molecules (T_g) and electron (T_e) are in same range $T_e \approx T_g$, that is why thermal plasmas are also known as equilibrium plasmas (Boulos *et al.*, 2016). Thermal plasma is being considered low-economical due to higher input energy, installation cost and difficult to handle due to high reactor temperature and controlled pressure (Toth *et al.*, 2016). Thermal plasma is suitable for the production of liquids fuels, in gas phase processes, the high temperature can erode the high voltage (HV) electrode (Du *et al.*, 2015). The thermal plasma possessing high energy electron having 10 eV with the density of almost $10^5 e^{-m^{-3}}$. The temperature is considerably high i.e. 5×10^3 to 5×10^4 K (Locke *et al.*, 2006). Thermal plasma producing a higher yield of CO and H_2 (Bromberg *et al.*, 1998; Lee *et al.*, 2010). Nevertheless, the consumption of high energy 10 to 20 MJ-kg⁻¹ H_2 and the power density 4 kW-L⁻¹ are the main concerns for thermal plasma DRM process (Bromberg *et al.*, 1998; Liu *et al.*, 2010).

NTP is considered as the most suitable technology for the DRM due to its non-thermal equilibrium properties, simple design and lower energy consumption (Eliasson *et al.*, 2000; Lu *et al.*, 2017). Among the NTPs, dielectric barrier discharge (DBD) is more promising for DRM due to its lower energy consumption, simple design and low installation cost (Paulmier and Fulcheri, 2005; Snoeckx and Bogaerts, 2017). Since, DBD plasma operates at room temperature and atmospheric pressure, easy to operate and feedstock versatility makes a more attractive approach

for DRM (Snoeckx *et al.*, 2016b). DBD could generate high energetic species consists of electrons, neutrons, radicals and ions; that excite, ionize and dissociate CH₄ and CO₂ to final products (Eliasson *et al.*, 2000; Kogelschatz, 2003; Li *et al.*, 2007). DBD can be constructed planer and cylindrical orientation using a dielectric material to separate by two electrodes, HV electrode and ground electrode creating a potential difference and accelerate electrons from anode to cathode which creates an electric field. The electrons dissociate the reactant gases and convert into products.

Numerous studies have been undertaken to investigate DRM using DBD plasma at various experimental conditions (Aghamir *et al.*, 2004; Chung *et al.*, 2014; Krawczyk *et al.*, 2014; Wang *et al.*, 2009b) to convert CH₄ and CO₂ to valuable fuels like syngas and higher hydrocarbons (HCs). On the other hand, DBD plasma performance is dependent some of leading process parameters i.e., feed flow rate, feed molar ratio, input power, catalyst loading and reactor temperature (Neyts *et al.*, 2015; Usman *et al.*, 2015; Xin *et al.*, 2011; Yap *et al.*, 2015). Although, DBD plasma has been successfully investigated for DRM application with an appreciable number of desired products, yet foremost concern is the power dissipation, low energy efficiency (EE) and carbon deposition due to methane cracking and Boudouard reactions (Equations 1.2 -1.3). The deposited carbon deactivates the active sites of the catalyst and sometimes leads to the reactor blockage.



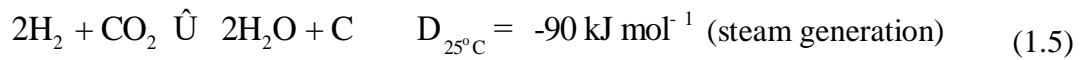
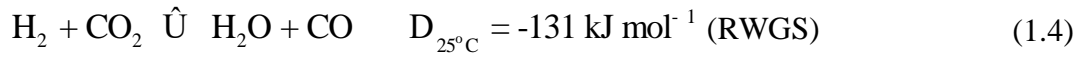
To improve the EE and inhibit the carbon formation problem, researchers introduced various catalyst systems to overcome the carbon formation and achieve higher stability in DRM (Brune *et al.*, 2018). The majorly used catalyst are Ni-based due to cheaply available (Pakhare and Spivey, 2014). Another approach which is being practiced currently to synthesise a catalyst using transition and noble metals such as La, Ce, Pt, Rh, Ru, Pd on different supports such as Al₂O₃, SiO₂, SBA, MgO,

MCM and TiO_3 (Fan *et al.*, 2011a; Guo *et al.*, 2015b; Nair and Kaliaguine, 2016; Tu *et al.*, 2011b; Zhu *et al.*, 2008a). Transition and noble metals displayed high catalytic activity along with high resistant to coke deposition (Khani *et al.*, 2016). However, transition and noble metals are expensive compared to conventional non-noble metals. Now by looking into elementary problem, it is required to synthesize a stable catalyst, which can exhibit high resistance to coke deposition and stability towards DRM activity in DBD plasma. The selection of the catalyst must be based on better physico-chemical properties and availability. Keeping in mind, Ni, Mg and Al are available abundantly in earth crust and Al having high surface area, while transition metal like La or Ce can be accommodated in a small amount as co-support to achieve the high stability (Li *et al.*, 2017b). MgAl_2O_4 has been used for thermal-DRM previously and reported a good activity towards conversion and selectivity (Damyanova *et al.*, 2012; Habibi *et al.*, 2016b). MgAl_2O_4 easily can be modified using co-support to enhance its performance and more resistance to coke. MgAl_2O_4 has been reported as strong basic support and it has not been used the DBD plasma DRM. It may be interesting to investigate MgAl_2O_4 incorporated with co-support to achieve the stability and coke resistance in DBD DRM.

1.2 Problem Statement

Although, recycling of greenhouse gases (CO_2 and CH_4) into valuable chemicals is an attractive approach to mitigate global warming, breaking stable molecules of CO_2 and CH_4 is a major challenge (Indarto *et al.*, 2008; OECD, 2015; Song, 2002). Among the known technologies, NTP via DBD reactor is the most attractive approach for DRM due to the easy handling, low installation cost and low temperature and pressure operations (Indarto *et al.*, 2008; Jo *et al.*, 2015; Nozaki *et al.*, 2017; Zhou *et al.*, 1998). However, low conversion, selectivity and EE have been reported in DBD plasma DRM and addition of rapid coke formation via Equation 1.2 and 1.3. Due to the carbon deposition, the active site of catalyst are blocked which deactivate catalyst and conversion efficiency reduced to a very unacceptable situation (Pakhare and Spivey, 2014). Coke formation in DBD plasma DRM is the

critical problem identified by many researchers which can be overcome by introducing stable catalysts (Aw *et al.*, 2015). The carbon formation and other reactions like reverse water gas shift (RWGS) (Equation 1.4) reaction, steam generation via DRM (Equation 1.5) made the syngas (H₂/CO) ratio lower than unity. It is inappropriate for further utilisation for downstream processing for liquid fuels via Fischer-Tropsch (FT) synthesis (Maitlis and de Klerk, 2013).



Among the known catalysts, Ni-base catalysts are the most widely researched material due to low cost, availability and prolonged stability. However, it has been observed lower conversion with lesser products selectivity in Ni-based catalyst (Hafez *et al.*, 2015) due to the rapid carbon formation on the tip of Ni particles. The noble metals like Pt, Rh, Pd, Ru, are displaying high resistance towards coking but the cost is very high and nearly unacceptable for industrial utilisation (Doghachi *et al.*, 2016). Rare earth metals such as La and Ce have high stability in thermal DRM. The Ni/Al₂O₃ and MgO has been used for DBD plasma DRM. Ni/Al₂O₃ exhibited excessive coke formation and Ni/MgO has low catalytic activity, although it resists to coking to some extent due to its basicity (Ganesh, 2013). Then MgAl₂O₄ has been synthesised to achieve high surface area and high basicity but the stability was still uncertain. The efficiency of Ni-based MgAl₂O₄ supported catalyst could be enhanced by modifying its structure with different rare earth metal oxides like La₂O₃ as co-support. MgAl₂O₄ has been solely used in thermal-DRM and reported a better choice for high CO₂ conversion (Zhao *et al.*, 2013). However, up to date no modification of MgAl₂O₄ using La₂O₃ as co-support is not stated. Moreover, the preparation methods are also responsible for the major properties like surface area, metal dispersion, basicity, and stability of the catalyst (Muraleedharan and Kaliaguine, 2016).

On the other hand, catalytic DBD plasma reactor is considered as low energy efficient system due to the loopholes in reactor design (Chung and Chang, 2016b).

The most commonly used catalytic DBD reactors are cylindrical fixed bed reactor. The specific design parameters such as discharge gap (D_{gap}), discharge length (D_L), discharge volume (V_D) have not been systematically studied for DBD plasma reactor. The reactor configuration study should have been studied exclusively, suggested by (Awadallah *et al.*, 2014) which can enhance the EE of the DBD plasma reactor. Furthermore, the catalyst incorporation in the DBD reactor is also a challenging task during the calculation of gas hourly space velocity GHSV (h^{-1}) along the V_D (Montoro-Damas *et al.*, 2015). The packing material may also influence the discharge chemistry of DBD plasma which is reported by Jo *et al.* (2013).

Apart from catalyst incorporation in DBD plasma reactor, the effects of dielectric material (reactor tube) on DRM activity has not been systematically studied. Previous studies advocated that dielectric material has a substantial effect on the plasma chemistry (Ozkan *et al.*, 2016a) and affected activity in plasma-based DRM process (Li *et al.*, 2004b). Till date now there is no report published to examine dielectric material performance in DBD plasma DRM activity. Finally, the stability and the H_2/CO ratio is one of the leading problems in DBD DRM to discourse. It is important to figure out the temperature effect in gas heating in DBD plasma to understand its effect on activation energy (E_a).

1.3 Research Hypothesis

The development of a new catalyst required to inhibit coke formation, strong thermal stability and enhance the products selectivity. It is hypothesized that DBD plasma reactor EE could be enhanced using a modified MgAl_2O_4 catalyst which has been identified as high basic nature catalyst and tolerant to carbon deposition (Habibi *et al.*, 2016b). Recently, MgAl_2O_4 spinel with the high surface area and high basicity has been synthesized for DRM (Guo *et al.*, 2004; Wei *et al.*, 2018). However, the catalyst exhibited low stability without the addition of any active metals or co-support. Addition of active metal improves the catalytic activity but stability is still a major challenge in plasma DRM processes (Messaoudi *et al.*, 2018).

La₂O₃ has shown high stability in thermo-catalytic DRM (Charisiou *et al.*, 2016). The rare earth metal-oxides used in DRM displayed a significant resistant towards carbon formation ascribed to the strong basic nature and carbon-gasification (Li *et al.*, 2017b; Zheng *et al.*, 2015b). La₂O₃ has been employed as a major support in the DRM process owing to its strong basic nature and high metal dispersion capability. La₂O₃, as a mix-matrix support, can prevent the carbon deposition and prolongs catalyst stability owing to its ability to react with CO₂ to form intermediate carbonate La₂O₂CO₃ (Liu *et al.*, 2016b; Zeng *et al.*, 2017). The catalytic performance of Ni-impregnated MgAl₂O₄ may be improved by adding La₂O₃ as co-support. The Ni interaction with MgAl₂O₄ could be enhanced by the combined effect of Al and Mg as well as subsequent assistance from La₂O₃ (Li *et al.*, 1992). It is envisaged that the incorporation of La₂O₃ and MgAl₂O₄ as mixed-support can enhance the basicity of catalyst, resist Ni particles agglomeration and curtail carbon formation (Al-Fatesh *et al.*, 2014; Li *et al.*, 2017a). Therefore, it is appropriate to synthesize and examine the role of La₂O₃ as co-support in Ni-impregnated MgAl₂O₄ in a catalytic-DBD plasma DRM. Recycling or regeneration of the proposed catalyst is highly possible using oxygen and nitrogen as a reducing and purging agent. It may reduce the formed carbon filaments and carbonates to their original states (Lee *et al.*, 2018). The preparation method of the catalyst has a significant influence on the structure/morphology and activity of the material. The materials are prepared using modified co-precipitation followed by hydrothermal method (Li *et al.*, 2017b) shows better structure and stability.

The reactor configuration can contribute in EE of the DBD reactor. The parameters like D_{gap} , D_L and V_D can play a significant role in the performance of the reactor. As these parameters are associated with gas processing capacity including specific input energy (SIE) and EE of DBD reactor (Montoro-Damas *et al.*, 2015). The dielectric material can also play a significant role in DBD plasma performance. It is evident the performance of a DBD reactor is related to the characteristics of the dielectric materials. The materials having high dielectric constant and more resistant to high temperature are considered more suitable for a DBD reactor to hinder power dissipation (Ozkan *et al.*, 2016c). The properties of dielectric material i.e., dielectric constant, morphology and temperature tolerance are the key parameters to consider.

By incorporating the proposed catalyst in a systematic studied DBD reactor, the higher EE, higher H₂/CO ratio and stability is highly expected. The synergistic effect of the plasma-catalysis is vastly targeted in the proposed study.

1.4 Research Objectives

Considering the identified major problems in catalytic-DBD DRM, the main objectives of the present study are follows:

- i. To synthesise and characterise of Ni loaded La₂O₃-MgAl₂O₄ nano-catalyst for DBD plasma DRM.
- ii. To investigate the reactor configuration and dielectric material effect in DBD plasma reactor for DRM.
- iii. To investigate the catalytic activity, selectivity and regeneration capability of Ni/La₂O₃-MgAl₂O₄ catalyst for DBD plasma DRM.
- iv. To optimise process parameter of catalytic-DBD plasma DRM using multiple response surface methodology.
- v. To examine the kinetic parameters of catalytic-DBD plasma DRM and fluid modelling for plasma discharge characteristics.

1.5 Scope of the Study

The Ni/La₂O₃-MgAl₂O₄ nano-composite is prepared by modified co-precipitation method, followed by hydrothermal process. La₂O₃/MgAl₂O₄ is prepared by microemulsion method then impregnated Ni over the mixed-matrix support and calcined. For the sake of comparison, the γ -Al₂O₃, 10% Ni/ γ -Al₂O₃, 10% Ni/MgO, 10% Ni/ γ -Al₂O₃-MgO, MgAl₂O₄ and 10% Ni/MgAl₂O₄ prepared and tested in DBD plasma DRM. Ni loading (5-20 %) was investigated to evaluate the plasma-catalytic activity. Detailed characterisation was carried-out to check the physico-chemical

properties of the synthesised catalyst. The prepared samples will be characterized by nitrogen adsorption-desorption (BET), X-ray diffraction (XRD), Raman spectra, Fourier transform infrared spectroscopy (FTIR), H₂-temperature programmed reduction (H₂-TPR) and CO₂-temperature programmed desorption (CO₂-TPD), field emission scanning electron microscopy (FE-SEM), energy-dispersive X-ray spectroscopy (EDX), transmission electron microscopy (TEM), thermogravimetric analysis (TGA) and dielectric properties. The dielectric properties of the prepared samples were analysed to know the dielectric constant of the catalyst. The DBD plasma reactor is used for DRM to analyse the catalytic activity of the prepared catalyst.

In reactor configuration, D_{gap} , D_L , V_D and catalyst packing were investigated for DBD reactor using prepared samples. The performance of the two different dielectric materials (quartz and alumina) were examined in DBD plasma for different parameters such as GHSV, SIE, feed ratio, and V_D . The reactor configuration such as D_{gap} , and D_L are directly used for the calculation of discharge volume. V_D has a direct relation with GHSV and EE. The prepared samples such as γ -Al₂O₃, Ni/ γ -Al₂O₃, Ni/MgO, Ni/ γ -Al₂O₃-MgO, MgAl₂O₄, Ni/MgAl₂O₄ and Ni/La₂O₃-MgAl₂O₄ respectively. Various Ni loadings were tested to check the effect on the DBD-DRM. The process parameters optimization was carried out using RSM to investigate the effect of process variables such as flow rate, feed ratio, input power and catalyst loading the conversion of CH₄ and CO₂ as well as the selectivity of products and EE of DBD plasma DRM. The kinetic study was carried out using Power-law model to investigate the rate constants (k) and rate of conversion (X) using Ni/La₂O₃-MgAl₂O₄. The COMSOL Multiphysics software was used to investigate the electric properties of Argon-based DBD reactor.

1.6 Significance of the Research

The synthesis of high basic Ni/La₂O₃-MgAl₂O₄ shows high catalytic activity and stability in the catalytic-DBD plasma DRM. The regeneration capability of the synthesized material is considered a key step towards the stability of the DBD

plasma DRM process. The H_2/CO is unity in the presented study, a substantial prospective for further utilization in FT synthesis for liquid fuel production. The systematic reactor configuration (DBD reactor) study is investigated to oversee the contribution in the EE of DBD plasma. The reactor configuration study shows the EE can be improved via optimizing the geometric parameters. The kinetic study based on reactor configuration is proposed using Power-law model. The plasma characteristics of the Ar-DBD is presented using fluid modelling approach for various dielectric constant and D_{gap} .

1.7 Organization of the Study

The organization of the study is composed of 8 Chapters. The research background, research problem, research hypothesis, scope and significance of the study is presented in Chapter 1. The extensive literature review on DRM process, catalytic-DBD plasma reactor study, catalyst systems and literature on kinetic and fluid modelling study is drafted in Chapter 2. Chapter 3 provides the research methodology adopted in this study: material synthesis, characterization, reactor setup, catalytic activity calculations, process optimization and kinetic study basic descriptions. Chapter 4 deals with the detail characterization of the synthesized material using various techniques. The DBD reactor design and performance of the material is presented in Chapter 5. Process optimization using RSM is provided in Chapter 6. Chapter 7 is divided into two parts: (i) The macroscopic kinetic study of catalytic-DBD plasma DRM (ii) The fluid modelling study of Ar-based DBD. The conclusion and recommendations of the study is provided in Chapter 8.

REFERENCES

- Abdollahifar, M., Haghghi, M. and Babaluo, A. A. (2014). Syngas production via dry reforming of methane over Ni/Al₂O₃-MgO nanocatalyst synthesized using ultrasound energy. *Journal of Industrial and Engineering Chemistry*. 20 (4), 1845-1851.
- Abdullah, B., Ghani, N. A. A. and Vo, D. V. N. (2017). Recent advances in dry reforming of methane over Ni-based catalysts. *Journal of Cleaner Production*. 162, 170-185.
- Aboul-Gheit, A. K. (2007). The role of additives in the impregnation of platinum and ruthenium on alumina catalysts. *Journal of Chemical Technology and Biotechnology*. 29 (8), 480-486.
- Aerts, R., Somers, W. and Bogaerts, A. (2015). Carbon dioxide splitting in a dielectric barrier discharge plasma: a combined experimental and computational study. *ChemSusChem*. 8 (4), 702-716.
- Aghamir, F. M., Matin, N. S., Jalili, A. H., Esfarayeni, M. H., Khodagholi, M. A. and Ahmadi, R. (2004). Conversion of methane to methanol in an ac dielectric barrier discharge. *Plasma Sources Science and Technology*. 13 (4), 707.
- Ahmad, S., Wong, K. Y., Tseng, M. L. and Wong, W. P. (2018). Sustainable product design and development: A review of tools, applications and research prospects. *Resources, Conservation and Recycling*. 132, 49-61.
- Ahmed, W., Awadallah, A. E. and Aboul-Enein, A. A. (2016). Ni/CeO₂-Al₂O₃ catalysts for methane thermo-catalytic decomposition to CO_x-free H₂ production. *International Journal of Hydrogen Energy*. 41 (41), 18484-18493.
- Akbari, E., Alavi, S. M. and Rezaei, M. (2017). Synthesis gas production over highly active and stable nanostructured Ni MgO Al₂O₃ catalysts in dry reforming of methane: Effects of Ni contents. *Fuel*. 194, 171-179.
- Akri, M., Chafik, T., Granger, P., Ayrault, P. and Batiot-Dupeyrat, C. (2016). Novel nickel promoted illite clay based catalyst for autothermal dry reforming of methane. *Fuel*. 178, 139-147.
- Al-Fatesh, A. S., Naeem, M. A., Fakeeha, A. H. and Abasaheed, A. E. (2013). CO₂

- reforming of methane to produce syngas over γ -Al₂O₃-supported Ni–Sr catalysts. *Bulletin of the Chemical Society of Japan*. 86 (6), 742-748.
- Al-Fatesh, A. S., Naeem, M. A., Fakeeha, H. and Abasaheed, A. E. (2014). Role of La₂O₃ as promoter and support in Ni/gamma-Al₂O₃ catalysts for dry reforming of methane. *Chinese Journal of Chemical Engineering*. 22 (1), 28-37.
- Alipour, Z., Rezaei, M. and Meshkani, F. (2014). Effect of Ni loadings on the activity and coke formation of MgO-modified Ni/Al₂O₃ nanocatalyst in dry reforming of methane. *Journal of Energy Chemistry*. 23 (5), 633-638.
- Alliati, M., Mei, D. and Tu, X. (2018). Plasma activation of CO₂ in a dielectric barrier discharge: A chemical kinetic model from the microdischarge to the reactor scales. *Journal of CO2 Utilization*. 27, 308-319.
- Alves, L., Bogaerts, A., Guerra, V. and Turner, M. (2018). Foundations of modelling of nonequilibrium low-temperature plasmas. *Plasma Sources Science and Technology*. 27 (2), 023002.
- Antonin, B. and Annemie, B. (2017). Modeling of CO₂ plasma: Effect of uncertainties in the plasma chemistry. *Plasma Sources Science and Technology*.
- Aw, M. S., Zorko, M., Osojnik Črnivec, I. G. and Pintar, A. (2015). Progress in the synthesis of catalyst supports: Synergistic effects of nanocomposites for attaining long-term stable activity in CH₄–CO₂ dry reforming. *Industrial & Engineering Chemistry Research*. 54 (15), 3775-3787.
- Awadallah, A. E., Aboul-Enein, A. A. and Aboul-Gheit, A. K. (2014). Effect of progressive Co loading on commercial Co–Mo/Al₂O₃ catalyst for natural gas decomposition to CO_x-free hydrogen production and carbon nanotubes. *Energy Conversion and Management*. 77, 143-151.
- Ayodele, B., Khan, M. R., Nooruddin, S. S. and Cheng, C. K. (2017). Modelling and optimization of syngas production by methane dry reforming over samarium oxide supported cobalt catalyst: response surface methodology and artificial neural networks approach. *Clean Technologies and Environmental Policy*. 19 (4), 1181-1193.
- Balusamy, B., Taştan, B. E., Ergen, S. F., Uyar, T. and Tekinay, T. (2015). Toxicity of lanthanum oxide (La₂ O₃) nanoparticles in aquatic environments. *Environmental Science: Processes & Impacts*. 17 (7), 1265-1270.

- Bell, T. E., Gonzalez-Carballo, J. M., Tooze, R. P. and Torrente-Murciano, L. (2015). Single-step synthesis of nanostructured γ -alumina with solvent reusability to maximise yield and morphological purity. [10.1039/C4TA06692H]. *Journal of Materials Chemistry A*. 3 (11), 6196-6201.
- Bogaerts, A., De Bie, C., Snoeckx, R. and Kozák, T. (2017). Plasma based CO₂ and CH₄ conversion: A modeling perspective. *Plasma Processes and Polymers*. 14 (6), 1600070.
- Bogaerts, A., Neyts, E., Gijbels, R. and van der Mullen, J. (2002). Gas discharge plasmas and their applications. *Spectrochimica Acta Part B-Atomic Spectroscopy*. 57 (4), 609-658.
- Bordoloi, A., Das, S., Goyal, R., Singha, R. K., Pendem, C. R., Narayan, S. K. L., Bal, R., Prasad, V. V. D. N., Botcha, N. N. and Kumar, M. (2017). Process for the preparation of Ni—CeMgAl₂O₄ catalyst for dry reforming of methane with carbon dioxide: Google Patents.
- Boulos, M. I., Fauchais, P. and Pfender, E. (2016). Basic Concepts of Plasma Generation *Handbook of Thermal Plasmas* (pp. 1-34). Cham: Springer International Publishing.
- Bromberg, L., Cohn, D. R., Rabinovich, A., O'Brien, C. and Hochgreb, S. (1998). Plasma reforming of methane. *Energy & Fuels*. 12 (1), 11-18.
- Brune, L., Ozkan, A., GENTY, E., de Bocarmé, T. V. and Reniers, F. (2018). Dry reforming of methane via plasma-catalysis: influence of the catalyst nature supported on alumina in a packed-bed DBD configuration. *Journal of Physics D: Applied Physics*.
- Charisiou, N. D., Siakavelas, G., Papageridis, K. N., Baklavaridis, A., Tzounis, L., Avraam, D. G. and Goula, M. A. (2016). Syngas production via the biogas dry reforming reaction over nickel supported on modified with CeO₂ and/or La₂O₃ alumina catalysts. *Journal of Natural Gas Science and Engineering*. 31, 164-183.
- Chawdhury, P., Ray, D. and Subrahmanyam, C. (2018). Single step conversion of methane to methanol assisted by nonthermal plasma. *Fuel Processing Technology*. 179, 32-41.
- Chen, G. X., Godfroid, T., Britun, N., Georgieva, V., Delplancke-Ogletree, M. P. and Snyders, R. (2017). Plasma-catalytic conversion of CO₂ and CO₂/H₂O in a

- surface-wave sustained microwave discharge. *Applied Catalysis B-Environmental*. 214, 114-125.
- Chen, H. L., Lee, H. M., Chen, S. H., Chao, Y. and Chang, M. B. (2008). Review of plasma catalysis on hydrocarbon reforming for hydrogen production-Interaction, integration, and prospects. *Applied Catalysis B-Environmental*. 85 (1-2), 1-9.
- Chen, H. W., Wang, C. Y., Yu, C. H., Tseng, L. T. and Liao, P. H. (2004). Carbon dioxide reforming of methane reaction catalyzed by stable nickel copper catalysts. *Catalysis Today*. 97 (2-3), 173-180.
- Choi, J. H., Il Lee, T., Han, I., Oh, B. Y., Jeong, M. C., Myoung, J. M., Baik, H. K., Song, K. M. and Lim, Y. S. (2006). Improvement of plasma uniformity using ZnO-coated dielectric barrier discharge in open air. *Applied Physics Letters*. 89 (8), 081501.
- Chowdhury, M. B., Sui, R., Lucky, R. A. and Charpentier, P. A. (2010). One-pot procedure to synthesize high surface area alumina nanofibers using supercritical carbon dioxide. *Langmuir*. 26 (4), 2707-2713.
- Chung, W.-C. and Chang, M.-B. (2016a). Review of catalysis and plasma performance on dry reforming of CH₄ and possible synergistic effects. *Renewable and Sustainable Energy Reviews*. 62 (Supplement C), 13-31.
- Chung, W. C. and Chang, M. B. (2016b). Dry reforming of methane by combined spark discharge with a ferroelectric. *Energy Conversion and Management*. 124, 305-314.
- Chung, W. C. and Chang, M. B. (2016c). Review of catalysis and plasma performance on dry reforming of CH₄ and possible synergistic effects. *Renewable & Sustainable Energy Reviews*. 62, 13-31.
- Chung, W. C., Pan, K. L., Lee, H. M. and Chang, M. B. (2014). Dry reforming of methane with dielectric barrier discharge and ferroelectric packed-bed reactors. *Energy & Fuels*. 28 (12), 7621-7631.
- Covert, T., Greenstone, M. and Knittel, C. R. (2016). Will We Ever Stop Using Fossil Fuels? *The Journal of Economic Perspectives*. 30 (1), 117-137.
- Cui, Y., Zhang, H., Xu, H. and Li, W. (2007). Kinetic study of the catalytic reforming of CH₄ with CO₂ to syngas over Ni/ α -Al₂O₃ catalyst: The effect of temperature on the reforming mechanism. *Applied Catalysis A: General*. 318, 79-88.

- Dahdah, E., Abou Rached, J., Aouad, S., Gennequin, C., Tidahy, H. L., Estephane, J., Aboukais, A. and Abi Aad, E. (2017). CO₂ reforming of methane over Ni_xMg_{6-x}Al₂ catalysts: Effect of lanthanum doping on catalytic activity and stability. *International Journal of Hydrogen Energy*. 42 (17), 12808-12817.
- Damyanova, S., Pawelec, B., Arishtirova, K. and Fierro, J. L. G. (2012). Ni-based catalysts for reforming of methane with CO₂. *International Journal of Hydrogen Energy*. 37 (21), 15966-15975.
- Dananjayan, R. R. T., Kandasamy, P. and Andimuthu, R. (2016). Direct mineral carbonation of coal fly ash for CO₂ sequestration. *Journal of Cleaner Production*. 112, 4173-4182.
- Danhua, M., Xinbo, Z., Ya-Ling, H., Joseph, D. Y. and Xin, T. (2015). Plasma-assisted conversion of CO₂ in a dielectric barrier discharge reactor: understanding the effect of packing materials. *Plasma Sources Science and Technology*. 24 (1), 015011.
- Das, S., Sengupta, M., Patel, J. and Bordoloi, A. (2017). A study of the synergy between support surface properties and catalyst deactivation for CO₂ reforming over supported Ni nanoparticles. *Applied Catalysis A-General*. 545 (Supplement C), 113-126.
- De Bie, C., Verheyde, B., Martens, T., van Dijk, J., Paulussen, S. and Bogaerts, A. (2011). Fluid modeling of the conversion of methane into higher hydrocarbons in an atmospheric pressure dielectric barrier discharge. *Plasma Processes and Polymers*. 8 (11), 1033-1058.
- Delikonstantis, E., Scapinello, M. and Stefanidis, G. (2017). Investigating the Plasma-Assisted and Thermal Catalytic Dry Methane Reforming for Syngas Production: Process Design, Simulation and Evaluation. *Energies*. 10 (9), 1429.
- Dincer, I. (2001). Environmental issues: I-energy utilization. *Energy Sources*. 23 (1), 69-81.
- Doghachi, F. A., Islam, A., Zainal, Z., Saiman, M. I., Embong, Z. and Taufiq, Y. Y. H. (2016). High coke-resistance Pt/Mg_{1-x}Ni_xO catalyst for dry reforming of methane. *PloS one*. 11 (1).
- Du, C., Mo, J. and Li, H. (2015). Renewable Hydrogen Production by Alcohols Reforming Using Plasma and Plasma-Catalytic Technologies: Challenges and Opportunities. *Chemical Reviews*. 115 (3), 1503-1542.

- Duan, X., Hu, Z., Li, Y. and Wang, B. (2015a). Effect of dielectric packing materials on the decomposition of carbon dioxide using DBD microplasma reactor. *AIChE Journal*. 61 (3), 898-903.
- Duan, X., Li, Y., Ge, W. and Wang, B. (2015b). Degradation of CO₂ through dielectric barrier discharge microplasma. *Greenhouse Gases: Science and Technology*. 5 (2), 131-140.
- Dybkjaer, I. and Aasberg-Petersen, K. (2016). Synthesis gas technology large-scale applications. *The Canadian Journal of Chemical Engineering*. 94 (4), 607-612.
- Effendi, A., Hellgardt, K., Zhang, Z. G. and Yoshida, T. (2003). Characterisation of carbon deposits on Ni/SiO₂ in the reforming of CH₄-CO₂ using fixed- and fluidised-bed reactors. *Catalysis Communications*. 4 (4), 203-207.
- Eliasson, B., Egli, W. and Kogelschatz, U. (1994). Modelling of dielectric barrier discharge chemistry. *Pure and applied chemistry*. 66 (6), 1275-1286.
- Eliasson, B. and Kogelschatz, U. (1991). Nonequilibrium Volume Plasma Chemical-Processing. *IEEE Transactions on Plasma Science*. 19 (6), 1063-1077.
- Eliasson, B., Liu, C. J. and Kogelschatz, U. (2000). Direct conversion of methane and carbon dioxide to higher hydrocarbons using catalytic dielectric-barrier discharges with zeolites. *Industrial & Engineering Chemistry Research*. 39 (5), 1221-1227.
- Erickson, R. W. and Maksimovic, D. (2007). *Fundamentals of power electronics*: Springer Science & Business Media.
- Estifae, P., Haghighi, M., Babaluo, A. A., Rahemi, N. and Jafari, M. F. (2014). The beneficial use of non-thermal plasma in synthesis of Ni/Al₂O₃-MgO nanocatalyst used in hydrogen production from reforming of CH₄/CO₂ greenhouse gases. *Journal of Power Sources*. 257, 364-373.
- Fan, M.-S., Abdullah, A. Z. and Bhatia, S. (2011a). Hydrogen production from carbon dioxide reforming of methane over Ni-Co/MgO-ZrO₂ catalyst: Process optimization. *International Journal of Hydrogen Energy*. 36 (8), 4875-4886.
- Fan, M. S., Abdullah, A. Z. and Bhatia, S. (2011b). Hydrogen production from carbon dioxide reforming of methane over Ni-Co/MgO-ZrO₂ catalyst: Process optimization. *International Journal of Hydrogen Energy*. 36 (8), 4875-4886.

- Fan, Z., Sun, K., Rui, N., Zhao, B. and Liu, C.-j. (2015). Improved activity of Ni/MgAl₂O₄ for CO₂ methanation by the plasma decomposition. *Journal of Energy Chemistry*. 24 (5), 655-659.
- Fang, X. Z., Lian, J., Nie, K. W., Zhang, X. H., Dai, Y. F., Xu, X. L., Wang, X., Liu, W. M., Li, C. Q. and Zhou, W. F. (2016). Dry reforming of methane on active and coke resistant Ni/Y₂Zr₂O₇ catalysts treated by dielectric barrier discharge plasma. *Journal of Energy Chemistry*. 25 (5), 825-831.
- Fauchais, P. and Rakowitz, J. (1979). Physics on plasma chemistry. *Le Journal de Physique Colloques*. 40 (C7), C7-289-C287-312.
- Fouskas, A., Kollia, M., Kambolis, A., Papadopoulou, C. and Matralis, H. (2014). Boron-modified Ni/Al₂O₃ catalysts for reduced carbon deposition during dry reforming of methane. *Applied Catalysis a-General*. 474, 125-134.
- Fridman, A. (2008). *Plasma chemistry*: Cambridge university press.
- Fuschillo, N., Lalevic, B. and Leung, B. (1974). Dielectric properties of NiO and NiO(Li). *Thin Solid Films*. 24 (1), 181-192.
- Gadkari, S., Tu, X. and Gu, S. (2017). Fluid model for a partially packed dielectric barrier discharge plasma reactor. *Physics of Plasmas*. 24 (9), 093510.
- Gallon, H. J., Tu, X., Twigg, M. V. and Whitehead, J. C. (2011). Plasma-assisted methane reduction of a NiO catalyst-Low temperature activation of methane and formation of carbon nanofibres. *Applied Catalysis B-Environmental*. 106 (3-4), 616-620.
- Gallon, H. J., Tu, X. and Whitehead, J. C. (2012). Effects of Reactor Packing Materials on H₂ Production by CO₂ Reforming of CH₄ in a Dielectric Barrier Discharge. *Plasma Processes and Polymers*. 9 (1), 90-97.
- Ganesh, I. (2013). A review on magnesium aluminate (MgAl₂O₄) spinel: synthesis, processing and applications. *International Materials Reviews*. 58 (2), 63-112.
- Gao, J., Hou, Z., Lou, H. and Zheng, X. (2011). Chapter 7 - Dry (CO₂) Reforming *Fuel Cells: Technologies for Fuel Processing* (pp. 191-221). Amsterdam: Elsevier.
- Gendy, T. S., El-Temtamy, S. A., Ghoneim, S. A., El-Salamony, R. A., El-Naggar, A. Y. and El-Morsi, A. K. (2016). Response surface methodology for carbon dioxide reforming of natural gas. *Energy Sources Part a-Recovery Utilization and Environmental Effects*. 38 (9), 1236-1245.
- Godinho, M., Goncalves, R. D., Leite, E. R., Raubach, C. W., Carreno, N. L. V.,

- Probst, L. F. D., Longo, E. and Fajardo, H. V. (2010). Gadolinium-doped cerium oxide nanorods: novel active catalysts for ethanol reforming. [journal article]. *Journal of Materials Science*. 45 (3), 593-598.
- González, A. G. and Herrador, M. Á. (2007). A practical guide to analytical method validation, including measurement uncertainty and accuracy profiles. *TrAC Trends in Analytical Chemistry*. 26 (3), 227-238.
- Goujard, V., Tatibouet, J. M. and Batiot-Dupeyrat, C. (2009). Use of a non-thermal plasma for the production of synthesis gas from biogas. *Applied Catalysis A-General*. 353 (2), 228-235.
- Groen, J. C., Peffer, L. A. A. and Perez-Ramirez, J. (2003). Pore size determination in modified micro- and mesoporous materials. Pitfalls and limitations in gas adsorption data analysis. *Microporous and Mesoporous Materials*. 60 (1-3), 1-17.
- Guler, M., Dogu, T. and Varisli, D. (2017). Hydrogen production over molybdenum loaded mesoporous carbon catalysts in microwave heated reactor system. *Applied Catalysis B-Environmental*. 219 (Supplement C), 173-182.
- Guo, F., Xu, J.-Q. and Chu, W. (2015a). CO₂ reforming of methane over Mn promoted Ni/Al₂O₃ catalyst treated by N₂ glow discharge plasma. *Catalysis Today*. 256 (Part 1), 124-129.
- Guo, F., Xu, J.-Q. and Chu, W. (2015b). CO₂ reforming of methane over Mn promoted Ni/Al₂O₃ catalyst treated by N₂ glow discharge plasma. *Catalysis Today*. 256, Part 1, 124-129.
- Guo, J., Lou, H., Zhao, H. and Zheng, X. (2005). Improvement of stability of out-layer MgAl₂O₄ spinel for a Ni/MgAl₂O₄/Al₂O₃ catalyst in dry reforming of methane. *Reaction Kinetics and Catalysis Letters*. 84 (1), 93-100.
- Guo, J. J., Lou, H., Zhao, H., Chai, D. F. and Zheng, X. M. (2004). Dry reforming of methane over nickel catalysts supported on magnesium aluminate spinels. *Applied Catalysis A-General*. 273 (1-2), 75-82.
- Guo, Y.-F., Ye, D.-Q., Chen, K.-F., He, J.-C. and Chen, W.-L. (2006). Toluene decomposition using a wire-plate dielectric barrier discharge reactor with manganese oxide catalyst in situ. *Journal of Molecular Catalysis A: Chemical*. 245 (1-2), 93-100.
- Guo, Y., Zou, J., Shi, X., Rukundo, P. and Wang, Z.-j. (2017). A Ni/CeO₂-CDC-SiC catalyst with improved coke resistance in CO₂ reforming of methane. *ACS*

Sustainable Chemistry & Engineering. 5 (3), 2330-2338.

- Gür, T. M. (2016). Comprehensive review of methane conversion in solid oxide fuel cells: Prospects for efficient electricity generation from natural gas. *Progress in Energy and Combustion Science*. 54, 1-64.
- Habibi, N., Arandiyan, H. and Rezaei, M. (2016a). Mesoporous MgO-Al₂O₃ nanopowder-supported meso-macroporous nickel catalysts: a new path to high-performance biogas reforming for syngas. [10.1039/C6RA01656A]. *RSC Advances*. 6 (35), 29576-29585.
- Habibi, N., Wang, Y., Arandiyan, H. and Rezaei, M. (2016b). Biogas Reforming for Hydrogen Production: A New Path to High-Performance Nickel Catalysts Supported on Magnesium Aluminate Spinel. *Chemcatchem*. 8 (23), 3600-3610.
- Hafez, K., Neda, Fathi, S., Shokri, B. and Hosseini, S. I. (2015). A novel method for decoking of Pt-Sn/Al₂O₃ in the naphtha reforming process using RF and pin-to-plate DBD plasma systems. *Applied Catalysis A: General*. 493, 8-16.
- Havran, V., Dudukovic, M. P. and Lo, C. S. (2011). Conversion of Methane and Carbon Dioxide to Higher Value Products. *Industrial & Engineering Chemistry Research*. 50 (12), 7089-7100.
- He, X. F., Hu, H. Q., Jin, L. J. and Hua, W. (2016). Integrated process of coal pyrolysis and CO₂ reforming of methane with and without using dielectric barrier discharge plasma. *Energy Sources Part A-Recovery Utilization and Environmental Effects*. 38 (5), 613-620.
- He, X. F., Jin, L. J., Wang, D., Zhao, Y. P., Zhu, S. W. and Hu, H. Q. (2011). Integrated Process of Coal Pyrolysis with CO₂ Reforming of Methane by Dielectric Barrier Discharge Plasma. *Energy & Fuels*. 25 (9), 4036-4042.
- He, Z., Liang, Z., Zhang, X. and Liu, C. (2017). Influence of copper nanowires grown in a dielectric layer on the performance of dielectric barrier discharge. *Journal of Vacuum Science & Technology B, Nanotechnology and Microelectronics: Materials, Processing, Measurement, and Phenomena*. 35 (1), 010603.
- Hensel, K., Katsura, S. and Mizuno, A. (2005). DC microdischarges inside porous ceramics. *IEEE Transactions on Plasma Science*. 33 (2), 574-575.
- Hensel, K., Martisovit, V., Machala, Z., Janda, M., Lestinsky, M., Tardiveau, P. and Mizuno, A. (2007). Electrical and optical properties of AC microdischarges

- in porous ceramics. *Plasma Processes and Polymers*. 4 (7-8), 682-693.
- Holzer, F., Kopinke, F. D. and Roland, U. (2005). Influence of ferroelectric materials and catalysts on the performance of non-thermal plasma (NTP) for the removal of air pollutants. *Plasma Chemistry and Plasma Processing*. 25 (6), 595-611.
- Holzer, F., Roland, U. and Kopinke, F. D. (2002). Combination of non-thermal plasma and heterogeneous catalysis for oxidation of volatile organic compounds: Part 1. Accessibility of the intra-particle volume. *Applied Catalysis B: Environmental*. 38 (3), 163-181.
- Hong, Y. C., Choi, D. H. and Chun, S. M. (2016). USA Patent No. US patents: K. Korea Basic Science Institute (Daejeon).
- Hou, Z. and Yashima, T. (2003). Small amounts of Rh-promoted Ni catalysts for methane reforming with CO₂. *Catalysis letters*. 89 (3), 193-197.
- Hussein, S., Zein, S. and Mohamed, A. R. (2004). Mn/Ni/TiO₂ catalyst for the production of hydrogen and carbon nanotubes from methane decomposition. *Energy & Fuels*. 18 (5), 1336-1345.
- Hwang, B. B., Yeo, Y. K. and Na, B. K. (2003). Conversion of CH₄ and CO₂ to syngas and higher hydrocarbons using dielectric barrier discharge. [journal article]. *Korean Journal of Chemical Engineering*. 20 (4), 631-634.
- Indarto, A., Choi, J.-W., Lee, H. and Song, H. K. (2006). Methane Conversion Using Dielectric Barrier Discharge: Comparison with Thermal Process and Catalyst Effects. *Journal of Natural Gas Chemistry*. 15 (2), 87-92.
- Indarto, A., Choi, J. W., Lee, H. and Song, H. K. (2008). Decomposition of greenhouse gases by plasma. [journal article]. *Environmental Chemistry Letters*. 6 (4), 215-222.
- Istadi, I. and Amin, N. A. S. (2007a). Modelling and optimization of catalytic-dielectric barrier discharge plasma reactor for methane and carbon dioxide conversion using hybrid artificial neural network - Genetic algorithm technique. *Chemical Engineering Science*. 62 (23), 6568-6581.
- Istadi, I. and Amin, N. A. S. (2007b). Modelling and optimization of catalytic-dielectric barrier discharge plasma reactor for methane and carbon dioxide conversion using hybrid artificial neural network—genetic algorithm technique. *Chemical Engineering Science*. 62 (23), 6568-6581.
- Izhab, I., Amin, N. A. S. and Asmadi, M. (2017). Dry Reforming of Methane over

- Oil Palm Shell Activated Carbon and ZSM-5 Supported Cobalt Catalysts. *International Journal of Green Energy*. null-null.
- Jabbour, K., El Hassan, N., Davidson, A., Casale, S. and Massiani, P. (2016). Factors affecting the long-term stability of mesoporous nickel-based catalysts in combined steam and dry reforming of methane. *Catalysis Science & Technology*. 6 (12), 4616-4631.
- Jean Marie, C. and Iulian, R. (2001). Syngas production via methane steam reforming with oxygen: plasma reactors versus chemical reactors. *Journal of Physics D: Applied Physics*. 34 (18), 2798.
- Jiang, T., Li, Y., Liu, C. J., Xu, G. H., Eliasson, B. and Xue, B. Z. (2002). Plasma methane conversion using dielectric-barrier discharges with zeolite A. *Catalysis Today*. 72 (3-4), 229-235.
- Jin, L. J., Li, Y., Lin, P. and Hu, H. Q. (2014). CO₂ reforming of methane on Ni/gamma-Al₂O₃ catalyst prepared by dielectric barrier discharge hydrogen plasma. *International Journal of Hydrogen Energy*. 39 (11), 5756-5763.
- Jo, S., Lee, D. H., Kang, W. S. and Song, Y. H. (2013). Effect of packing material on methane activation in a dielectric barrier discharge reactor. *Physics of Plasmas*. 20 (12), 123507.
- Jo, S., Lee, D. H., Kim, K. T., Kang, W. S. and Song, Y. H. (2014). Methane activation using Kr and Xe in a dielectric barrier discharge reactor. *Physics of Plasmas*. 21 (10), 103504.
- Jo, S., Lee, D. H. and Song, Y. H. (2015). Product analysis of methane activation using noble gases in a non-thermal plasma. *Chemical Engineering Science*. 130, 101-108.
- Jonathan, T., Sara, R., Christian, H., Lisa, T., Anuradha, V., Dolica, A.-E., Daniel, B. B., Anna, D., James, R. H., Dagmar, J., Sebastian, M., Keir, W.-L., Johannes, B., Ankur, A., Klaus, B., Annemie, B., Jean-Paul, B., Matthew, J. G., Khaled, H., Yukikazu, I., Bastiaan, J. B., Krishnakumar, E., Annarita, L., Nigel, J. M., Sumeet, P., Zoran Lj, P., Yi-Kang, P., Alok, R., Shahid, R., Julian, S., Miles, M. T., Peter, V., Whitehead, J. C. and Jung-Sik, Y. (2017). QDB: a new database of plasma chemistries and reactions. *Plasma Sources Science and Technology*. 26 (5), 055014.
- Kameshima, S., Tamura, K., Ishibashi, Y. and Nozaki, T. (2015). Pulsed dry methane reforming in plasma-enhanced catalytic reaction. *Catalysis Today*. 256, 67-

- Kameshima, S., Tamura, K., Mizukami, R., Yamazaki, T. and Nozaki, T. (2017). Parametric analysis of plasma-assisted pulsed dry methane reforming over Ni/Al₂O₃ catalyst. *Plasma Processes and Polymers*. 14 (6), 1600096.
- Kamonsuangkasem, K., Therdthianwong, S., Therdthianwong, A. and Thammajak, N. (2017). Remarkable activity and stability of Ni catalyst supported on CeO₂-Al₂O₃ via CeAlO₃ perovskite towards glycerol steam reforming for hydrogen production. *Applied Catalysis B-Environmental*. 218 (Supplement C), 650-663.
- Kang, J. G., Kim, Y. I., Cho, D. W. and Sohn, Y. (2015). Synthesis and physicochemical properties of La(OH)₃ and La₂O₃ nanostructures. *Materials Science in Semiconductor Processing*. 40 (Supplement C), 737-743.
- Kang, K.-M., Kim, H.-W., Shim, I.-W. and Kwak, H.-Y. (2011). Catalytic test of supported Ni catalysts with core/shell structure for dry reforming of methane. *Fuel Processing Technology*. 92 (6), 1236-1243.
- Karakaya, C. and Kee, R. J. (2016). Progress in the direct catalytic conversion of methane to fuels and chemicals. *Progress in Energy and Combustion Science*. 55, 60-97.
- Kathiraser, Y., Oernar, U., Saw, E. T., Li, Z. W. and Kawi, S. (2015). Kinetic and mechanistic aspects for CO₂ reforming of methane over Ni based catalysts. *Chemical Engineering Journal*. 278, 62-78.
- Kawi, S., Kathiraser, Y., Ni, J., Oemar, U., Li, Z. and Saw, E. T. (2015). Progress in Synthesis of Highly Active and Stable Nickel-Based Catalysts for Carbon Dioxide Reforming of Methane. *ChemSusChem*. 8 (21), 3556-3575.
- Kennedy, C., Steinberger, J., Gasson, B., Hansen, Y., Hillman, T., Havranek, M., Pataki, D., Phdungsilp, A., Ramaswami, A. and Villalba Mendez, G. (2009). Greenhouse gas emissions from global cities. *Environ Sci Technol*. 43 (19), 7297-7302.
- Khan, S. Z., Yuan, Y., Abdolvand, A., Schmidt, M., Crouse, P., Li, L., Liu, Z., Sharp, M. and Watkins, K. G. (2009). Generation and characterization of NiO nanoparticles by continuous wave fiber laser ablation in liquid. [journal article]. *Journal of Nanoparticle Research*. 11 (6), 1421-1427.
- Khani, Y., Shariatinia, Z. and Bahadoran, F. (2016). High catalytic activity and stability of ZnLaAlO₄ supported Ni, Pt and Ru nanocatalysts applied in the

- dry, steam and combined dry-steam reforming of methane. *Chemical Engineering Journal*. 299, 353-366.
- Khoja, A. H., Tahir, M. and Amin, N. A. S. (2017). Dry reforming of methane using different dielectric materials and DBD plasma reactor configurations. *Energy Conversion and Management*. 144, 262-274.
- Kim, A. R., Lee, H. Y., Lee, D. H., Kim, B. W., Chung, C. H., Moon, D. J., Jang, E. J., Pang, C. and Bae, J. W. (2015a). Combined Steam and CO₂ Reforming of CH₄ on LaSrNiOx, Mixed Oxides Supported on Al₂O₃-Modified SiC Support. *Energy & Fuels*. 29 (2), 1055-1065.
- Kim, H. and Ogata, A. (2012). Interaction of nonthermal plasma with catalyst for the air pollution control. *Int. J. Plasma Environ. Sci. Technol.* 6 (1), 43-48.
- Kim, H. H., Teramoto, Y., Negishi, N. and Ogata, A. (2015b). A multidisciplinary approach to understand the interactions of nonthermal plasma and catalyst: A review. *Catalysis Today*. 256, 13-22.
- Kim, H. J., Lee, H. C., Rhee, C. H., Chung, S. H., Lee, H. C., Lee, K. H. and Lee, J. S. (2003). Alumina nanotubes containing lithium of high ion mobility. *J Am Chem Soc*. 125 (44), 13354-13355.
- Kogelschatz, U. (2002). Dielectric-Barrier Discharges : Their History, Discharge Physics, and Industrial Applications. *Plasma Chemistry and Plasma Processing*. 23 (1), 1-46.
- Kogelschatz, U. (2003). Dielectric-barrier discharges: Their history, discharge physics, and industrial applications. *Plasma Chemistry and Plasma Processing*. 23 (1), 1-46.
- Kolb, T., Kroker, T., Voigt, J. H. and Gericke, K. H. (2012). Wet Conversion of Methane and Carbon Dioxide in a DBD Reactor. *Plasma Chemistry and Plasma Processing*. 32 (6), 1139-1155.
- Kraus, M., Eliasson, B., Kogelschatz, U. and Wokaun, A. (2001). CO₂ reforming of methane by the combination of dielectric-barrier discharges and catalysis. [10.1039/B007015G]. *Physical Chemistry Chemical Physics*. 3 (3), 294-300.
- Krawczyk, K., Mlotek, M., Ulejczyk, B. and Schmidt-Szalowski, K. (2014). Methane conversion with carbon dioxide in plasma-catalytic system. *Fuel*. 117, 608-617.
- Kundu, S. K., Kennedy, E. M., Gaikwad, V. V., Molloy, T. S. and Dlugogorski, B. Z. (2012). Experimental investigation of alumina and quartz as dielectrics for a

- cylindrical double dielectric barrier discharge reactor in argon diluted methane plasma. *Chemical Engineering Journal*. 180, 178-189.
- Lane, J. E. (2016). The COP-21 Agreement: A Giant Illusion? *Journal of Economics and Public Finance*. 2 (1), 34.
- Lashof, D. A. and Ahuja, D. R. (1990). Relative contributions of greenhouse gas emissions to global warming. *Nature*. 344 (6266), 529-531.
- Lavoie, J.-M. (2014). Review on dry reforming of methane, a potentially more environmentally-friendly approach to the increasing natural gas exploitation. *Frontiers in Chemistry*. 2, 81.
- Lee, D. H., Kim, K. T., Cha, M. S. and Song, Y. H. (2010). Plasma-controlled chemistry in plasma reforming of methane. *International Journal of Hydrogen Energy*. 35 (20), 10967-10976.
- Lee, H., Lee, D.-H., Ha, J. M. and Kim, D. H. (2018). Plasma assisted oxidative coupling of methane (OCM) over Ag/SiO₂ and subsequent regeneration at low temperature. *Applied Catalysis A: General*. 557, 39-45.
- Lee, H., Lee, D. H., Song, Y. H., Choi, W. C., Park, Y. K. and Kim, D. H. (2015). Synergistic effect of non-thermal plasma-catalysis hybrid system on methane complete oxidation over Pd-based catalysts. *Chemical Engineering Journal*. 259, 761-770.
- Lee, H. C., Kim, H. J., Chung, S. H., Lee, K. H., Lee, H. C. and Lee, J. S. (2003). Synthesis of unidirectional alumina nanostructures without added organic solvents. *J Am Chem Soc*. 125 (10), 2882-2883.
- Li, D. L., Li, R. L., Lu, M. M., Lin, X. Y., Zhan, Y. Y. and Jiang, L. L. (2017a). Carbon dioxide reforming of methane over Ru catalysts supported on Mg-Al oxides: A highly dispersed and stable Ru/Mg(Al)O catalyst. *Applied Catalysis B-Environmental*. 200, 566-577.
- Li, D. L., Nakagawa, Y. and Tomishige, K. (2011). Methane reforming to synthesis gas over Ni catalysts modified with noble metals. *Applied Catalysis a-General*. 408 (1-2), 1-24.
- Li, D. X., Pirouz, P., Heuer, A. H., Yadavalli, S. and Flynn, C. P. (1992). A high-resolution electron microscopy study of MgO/Al₂O₃ interfaces and MgAl₂O₄ spinel formation. *Philosophical Magazine A*. 65 (2), 403-425.
- Li, M.-w., Xu, G.-h., Tian, Y.-l., Chen, L. and Fu, H.-f. (2004a). Carbon dioxide reforming of methane using DC corona discharge plasma reaction. *The*

- Journal of Physical Chemistry A*. 108 (10), 1687-1693.
- Li, M. W., Tian, Y. L. and Xu, G. H. (2007). Characteristics of carbon dioxide reforming of methane via alternating current (AC) corona plasma reactions. *Energy & Fuels*. 21 (4), 2335-2339.
- Li, R., Tang, Q., Yin, S. and Sato, T. (2006). Plasma catalysis for CO₂ decomposition by using different dielectric materials. *Fuel Processing Technology*. 87 (7), 617-622.
- Li, R. X., Yamaguchi, Y., Shu, Y., Qing, T. and Sato, T. (2004b). Influence of dielectric barrier materials to the behavior of dielectric barrier discharge plasma for CO₂ decomposition. *Solid State Ionics*. 172 (1-4), 235-238.
- Li, W. Z., Kovarik, L., Mei, D. H., Liu, J., Wang, Y. and Peden, C. H. F. (2013). Stable platinum nanoparticles on specific MgAl₂O₄ spinel facets at high temperatures in oxidizing atmospheres. [Article]. *Nature Communications*. 4, 2481.
- Li, X. Y., Li, D., Tian, H., Zeng, L., Zhao, Z. J. and Gong, J. L. (2017b). Dry reforming of methane over Ni/La₂O₃ nanorod catalysts with stabilized Ni nanoparticles. *Applied Catalysis B-Environmental*. 202, 683-694.
- Lim, S. L., Lee, L. H. and Wu, T. Y. (2016). Sustainability of using composting and vermicomposting technologies for organic solid waste biotransformation: recent overview, greenhouse gases emissions and economic analysis. *Journal of Cleaner Production*. 111, 262-278.
- Liu, C., Ma, D., Ji, X., Zhao, S. and Li, S. (2011). Surfactant assisted synthesis of lamellar nanostructured LiFePO₄ at 388K. *Applied Surface Science*. 257 (9), 4529-4531.
- Liu, C., Mallinson, R. G. and Aresta, M. (2003). *Utilization of Greenhouse Gases*: American Chemical Society.
- Liu, C. J., Li, M. Y., Wang, J. Q., Zhou, X. T., Guo, Q. T., Yan, J. M. and Li, Y. Z. (2016a). Plasma methods for preparing green catalysts: Current status and perspective. *Chinese Journal of Catalysis*. 37 (3), 340-348.
- Liu, C. J., Xu, G. H. and Wang, T. M. (1999). Non-thermal plasma approaches in CO₂ utilization. *Fuel Processing Technology*. 58 (2-3), 119-134.
- Liu, C. J., Xue, B. Z., Eliasson, B., He, F., Li, Y. and Xu, G. H. (2001). Methane conversion to higher hydrocarbons in the presence of carbon dioxide using dielectric-barrier discharge plasmas. [journal article]. *Plasma Chemistry and*

- Plasma Processing*. 21 (3), 301-310.
- Liu, H., Da Costa, P., Hadj Taief, H. B., Benzina, M. and Gálvez, M. E. (2017). Ceria and zirconia modified natural clay based nickel catalysts for dry reforming of methane. *International Journal of Hydrogen Energy*. 42 (37), 23508-23516.
- Liu, H., Wierzbicki, D., Debek, R., Motak, M., Grzybek, T., Da Costa, P. and Gálvez, M. E. (2016b). La-promoted Ni-hydrotalcite-derived catalysts for dry reforming of methane at low temperatures. *Fuel*. 182, 8-16.
- Liu, K., Song, C. and Subramani, V. (2010). *Hydrogen and syngas production and purification technologies*: Wiley Online Library.
- Locke, B., Sato, M., Sunka, P., Hoffmann, M. and Chang, J.-S. (2006). Electrohydraulic discharge and nonthermal plasma for water treatment. *Industrial & engineering chemistry research*. 45 (3), 882-905.
- Loic, B., Alp, O., Eric, G., Thierry Visart de, B. and Francois, R. (2018). Dry reforming of methane via plasma-catalysis: influence of the catalyst nature supported on alumina in a packed-bed DBD configuration. *Journal of Physics D: Applied Physics*.
- Lu, J. F., Chen, Y., Ding, J. and Wang, W. L. (2016). High temperature energy storage performances of methane reforming with carbon dioxide in a tubular packed reactor. *Applied Energy*. 162, 1473-1482.
- Lu, N., Bao, X. D., Jiang, N., Shang, K. F., Li, J. and Wu, Y. (2017). Non-Thermal Plasma-Assisted Catalytic Dry Reforming of Methane and Carbon Dioxide Over g-C₃N₄-Based Catalyst. [journal article]. *Topics in Catalysis*. 60 (12-14), 855-868.
- Mahammadunnisa, S., Manoj Kumar Reddy, P., Ramaraju, B. and Subrahmanyam, C. (2013). Catalytic nonthermal plasma reactor for dry reforming of methane. *Energy & Fuels*. 27 (8), 4441-4447.
- Maitlis, P. M. and de Klerk, A. (2013). *Greener Fischer-Tropsch Processes for Fuels and Feedstocks*: John Wiley & Sons.
- Mao, S., Tan, Z., Zhang, L. and Huang, Q. (2018). Plasma-assisted biogas reforming to syngas at room temperature condition. *Journal of the Energy Institute*. 91 (2), 172-183.
- Matra, K. and Wongkuan, S. (2016). Non-thermal dielectric barrier discharge generator. *2016 International Electrical Engineering Congress, Ieecon2016*.

86, 313-316.

- Mei, D., Ashford, B., He, Y.-L. and Tu, X. (2017a). Plasma-catalytic reforming of biogas over supported Ni catalysts in a dielectric barrier discharge reactor: Effect of catalyst supports. *Plasma Processes and Polymers*. 14 (6), 1600076.
- Mei, D. and Tu, X. (2017). Conversion of CO₂ in a cylindrical dielectric barrier discharge reactor: Effects of plasma processing parameters and reactor design. *Journal of CO₂ Utilization*. 19, 68-78.
- Mei, D., Zhu, X., He, Y.-L., Yan, J. D. and Tu, X. (2014). Plasma-assisted conversion of CO₂ in a dielectric barrier discharge reactor: understanding the effect of packing materials. *Plasma Sources Science and Technology*. 24 (1), 015011.
- Mei, D., Zhu, X., He, Y.-L., Yan, J. D. and Tu, X. (2015). Plasma-assisted conversion of CO₂ in a dielectric barrier discharge reactor: understanding the effect of packing materials. *Plasma Sources Science and Technology*. 24 (1), 015011.
- Mei, D. H., Liu, S. Y. and Tu, X. (2017b). CO₂ reforming with methane for syngas production using a dielectric barrier discharge plasma coupled with Ni/γ-Al₂O₃ catalysts: Process optimization through response surface methodology. *Journal of CO₂ Utilization*. 21, 314-326.
- Messaoudi, H., Thomas, S., Djaidja, A., Slyemi, S. and Barama, A. (2018). Study of La_xNiO_y and La_xNiO_y/MgAl₂O₄ catalysts in dry reforming of methane. *Journal of CO₂ Utilization*. 24, 40-49.
- Michielsen, I., Uytendhouwen, Y., Pype, J., Michielsen, B., Mertens, J., Reniers, F., Meynen, V. and Bogaerts, A. (2017). CO₂ dissociation in a packed bed DBD reactor: First steps towards a better understanding of plasma catalysis. *Chemical Engineering Journal*.
- Montoro-Damas, A. M., Brey, J. J., Rodriguez, M. A., Gonzalez-Elipse, A. R. and Cotrino, J. (2015). Plasma reforming of methane in a tunable ferroelectric packed-bed dielectric barrier discharge reactor. *Journal of Power Sources*. 296, 268-275.
- Moreau, M., Orange, N. and Feuilloley, M. G. (2008). Non-thermal plasma technologies: new tools for bio-decontamination. *Biotechnol Adv*. 26 (6), 610-617.
- Muraleedharan, N., Mahesh and Kaliaguine, S. (2016). Structured catalysts for dry

- reforming of methane. *New J. Chem.* 40 (5), 4049-4060.
- Naeem, M. A., Al-Fatesh, A. S., Khan, W. U., Abasaeed, A. E. and Fakeeha, A. H. (2013). Syngas Production from Dry Reforming of Methane over Nano Ni Polyol Catalysts. *International Journal of Chemical Engineering and Applications*. 315-320.
- Nagaraja, B. M., Bulushev, D. A., Beloshapkin, S. and Ross, J. R. H. (2011). The effect of potassium on the activity and stability of Ni-MgO-ZrO₂ catalysts for the dry reforming of methane to give synthesis gas. *Catalysis Today*. 178 (1), 132-136.
- Nair, M. M. and Kaliaguine, S. (2016). Structured catalysts for dry reforming of methane. *New Journal of Chemistry*. 40 (5), 4049-4060.
- Nassar, M. Y., Ahmed, I. S. and Samir, I. (2014). A novel synthetic route for magnesium aluminate (MgAl₂O₄) nanoparticles using sol-gel auto combustion method and their photocatalytic properties. *Spectrochimica Acta Part A: Molecular and Biomolecular Spectroscopy*. 131, 329-334.
- Neyts, E. and Bogaerts, A. (2014). Understanding plasma catalysis through modelling and simulation—a review. *Journal of Physics D: Applied Physics*. 47 (22), 224010.
- Neyts, E. C. (2016). Plasma-Surface Interactions in Plasma Catalysis. [journal article]. *Plasma Chemistry and Plasma Processing*. 36 (1), 185-212.
- Neyts, E. C., Ostrikov, K. K., Sunkara, M. K. and Bogaerts, A. (2015). Plasma catalysis: Synergistic effects at the nanoscale. *Chemical Reviews*. 115 (24), 13408-13446.
- Nguyen, D. B. and Lee, W. G. (2015a). Analytical Approach to estimate and Predict the CO₂ Reforming of CH₄ in a Dielectric Barrier Discharge. *Chemical Engineering Communications*. 203 (7), 917-923.
- Nguyen, D. B. and Lee, W. G. (2015b). Comparison of different applied voltage waveforms on CO₂ reforming of CH₄ in an atmospheric plasma system. *Korean Journal of Chemical Engineering*. 32 (1), 62-67.
- Nguyen, H. H. and Kim, K.-S. (2015). Combination of plasmas and catalytic reactions for CO₂ reforming of CH₄ by dielectric barrier discharge process. *Catalysis Today*. 256, Part 1, 88-95.
- Ni, J., Chen, L., Lin, J., Schreyer, M. K., Wang, Z. and Kawi, S. (2013). High performance of Mg-La mixed oxides supported Ni catalysts for dry

- reforming of methane: The effect of crystal structure. *International Journal of Hydrogen Energy*. 38 (31), 13631-13642.
- Nishikawa, H., Kawamoto, D., Yamamoto, Y., Ishida, T., Ohashi, H., Akita, T., Honma, T., Oji, H., Kobayashi, Y., Hamasaki, A., Yokoyama, T. and Tokunaga, M. (2013). Promotional effect of Au on reduction of Ni(II) to form Au-Ni alloy catalysts for hydrogenolysis of benzylic alcohols. *Journal of Catalysis*. 307 (Supplement C), 254-264.
- Nozaki, T., Abe, S., Moriyama, S., Kameshima, S., Okazaki, K., Goujard, V. and Ağır, A. (2015). One step methane conversion to syngas by dielectric barrier discharge. *Japanese Journal of Applied Physics*. 54 (1S), 01AG01.
- Nozaki, T., Bogaerts, A., Tu, X. and Sanden, R. (2017). Special issue: Plasma Conversion. *Plasma Processes and Polymers*. 14 (6), 1790061.
- Ocsachoque, M. A., Aparicio, M. S. L. and Gonzalez, M. G. (2017). Effect of Rh addition to Ni/MgO-Al₂O₃ catalysts for dry reforming of methane. *Indian Journal of Science and Technology*. 10 (12).
- OECD. (2015). *CO₂ Emissions from Fuel Combustion* OECD Publishing.
- Omar, W. N. N. W. and Amin, N. A. S. (2011). Optimization of heterogeneous biodiesel production from waste cooking palm oil via response surface methodology. *Biomass & Bioenergy*. 35 (3), 1329-1338.
- Ozkan, A., Bogaerts, A. and Reniers, F. (2017). Routes to increase the conversion and the energy efficiency in the splitting of CO₂ by a dielectric barrier discharge. *Journal of Physics D-Applied Physics*. 50 (8), 084004.
- Ozkan, A., Dufour, T., Arnoult, G., De Keyzer, P., Bogaerts, A. and Reniers, F. (2015). CO₂-CH₄ conversion and syngas formation at atmospheric pressure using a multi-electrode dielectric barrier discharge. *Journal of CO₂ Utilization*. 9, 74-81.
- Ozkan, A., Dufour, T., Bogaerts, A. and Reniers, F. (2016a). How do the barrier thickness and dielectric material influence the filamentary mode and CO₂ conversion in a flowing DBD? *Plasma Sources Science and Technology*. 25 (4), 045016.
- Ozkan, A., Dufour, T., Silva, T., Britun, N., Snyders, R., Bogaerts, A. and Reniers, F. (2016b). The influence of power and frequency on the filamentary behavior of a flowing DBD—application to the splitting of CO₂. *Plasma Sources Science and Technology*. 25 (2), 025013.

- Ozkan, A., Dufour, T., Silva, T., Britun, N., Snyders, R., Reniers, F. and Bogaerts, A. (2016c). DBD in burst mode: solution for more efficient CO₂ conversion? *Plasma Sources Science and Technology*. 25 (5), 55005-55013.
- Padmaraj, O., Venkateswarlu, M. and Satyanarayana, N. (2015). Structural, electrical and dielectric properties of spinel type MgAl₂O₄ nanocrystalline ceramic particles synthesized by the gel-combustion method. *Ceramics International*. 41 (2, Part B), 3178-3185.
- Pakhare, D. and Spivey, J. (2014). A review of dry (CO₂) reforming of methane over noble metal catalysts. [10.1039/C3CS60395D]. *Chemical Society Reviews*. 43 (22), 7813-7837.
- Park, D., Kim, J. and Kim, T. (2018). Nonthermal plasma-assisted direct conversion of methane over NiO and MgO catalysts supported on SBA-15. *Catalysis Today*. 299, 86-92.
- Parker, R. W. R., Blanchard, J. L., Gardner, C., Green, B. S., Hartmann, K., Tyedmers, P. H. and Watson, R. A. (2018). Fuel use and greenhouse gas emissions of world fisheries. *Nature Climate Change*. 8 (4), 333-+.
- Patil, B. S., Cherkasov, N., Lang, J., Ibhaddon, A. O., Hessel, V. and Wang, Q. (2016). Low temperature plasma-catalytic NO_x synthesis in a packed DBD reactor: Effect of support materials and supported active metal oxides. *Applied Catalysis B-Environmental*. 194, 123-133.
- Paulmier, T. and Fulcheri, L. (2005). Use of non-thermal plasma for hydrocarbon reforming. *Chemical Engineering Journal*. 106 (1), 59-71.
- Paulussen, S., Verheyde, B., Tu, X., De Bie, C., Martens, T., Petrovic, D., Bogaerts, A. and Sels, B. (2010). Conversion of carbon dioxide to value-added chemicals in atmospheric pressure dielectric barrier discharges. *Plasma Sources Science & Technology*. 19 (3), 034015.
- Petitpas, G., Rollier, J. D., Darmon, A., Gonzalez-Aguilar, J., Metkemeijer, R. and Fulcheri, L. (2007). A comparative study of non-thermal plasma assisted reforming technologies. *International Journal of Hydrogen Energy*. 32 (14), 2848-2867.
- Pietruszka, B., Anklam, K. and Heintze, M. (2004). Plasma-assisted partial oxidation of methane to synthesis gas in a dielectric barrier discharge. *Applied Catalysis A: General*. 261 (1), 19-24.
- Pietruszka, B. and Heintze, M. (2004). Methane conversion at low temperature: the

- combined application of catalysis and non-equilibrium plasma. *Catalysis Today*. 90 (1-2), 151-158.
- Pinhao, N., Moura, A., Branco, J. B. and Neves, J. (2016). Influence of gas expansion on process parameters in non-thermal plasma plug-flow reactors: A study applied to dry reforming of methane. *International Journal of Hydrogen Energy*. 41 (22), 9245-9255.
- Pinhão, N. R., Janeco, A. and Branco, J. B. (2011). Influence of Helium on the Conversion of Methane and Carbon dioxide in a Dielectric Barrier Discharge. *Plasma Chemistry and Plasma Processing*. 31 (3), 427-439.
- Ponduri, S., Becker, M. M., Welzel, S., van de Sanden, M. C. M., Loffhagen, D. and Engeln, R. (2016). Fluid modelling of CO₂ dissociation in a dielectric barrier discharge. *Journal of Applied Physics*. 119 (9), 093301.
- Properties and applications of low-temperature plasma*. (1965). Springer US.
- Pu, Y.-K., Guo, Z.-G., Yu, Z.-D. and Ma, J. (2005). Tuning effect of inert gas mixing on electron energy distribution function in inductively coupled discharges. *Plasma physics and controlled fusion*. 48 (1), 61.
- Rahemi, N., Haghghi, M., Babaluo, A. A., Allahyari, S., Estifae, P. and Jafari, M. F. (2017). Plasma-Assisted Dispersion of Bimetallic Ni-Co over Al₂O₃-ZrO₂ for CO₂ Reforming of Methane: Influence of Voltage on Catalytic Properties. [journal article]. *Topics in Catalysis*. 60 (12-14), 843-854.
- Rahemi, N., Haghghi, M., Babaluo, A. A., Jafari, M. F. and Estifae, P. (2013a). CO₂ reforming of CH₄ over CeO₂-doped Ni/Al₂O₃ nanocatalyst treated by non-thermal plasma. *J Nanosci Nanotechnol*. 13 (7), 4896-4908.
- Rahemi, N., Haghghi, M., Babaluo, A. A., Jafari, M. F. and Estifae, P. (2013b). Synthesis and physicochemical characterizations of Ni/Al₂O₃-ZrO₂ nanocatalyst prepared via impregnation method and treated with non-thermal plasma for CO₂ reforming of CH₄. *Journal of Industrial and Engineering Chemistry*. 19 (5), 1566-1576.
- Ray, D., Manoj Kumar Reddy, P. and Challapalli, S. (2017a). Glass Beads Packed DBD-Plasma Assisted Dry Reforming of Methane. *Topics in Catalysis*. 1-10.
- Ray, D., Reddy, P. M. K. and Subrahmanyam, C. (2017b). Ni-Mn/ γ -Al₂O₃ assisted plasma dry reforming of methane. *Catalysis Today*.
- Ray, D. and Subrahmanyam, C. (2016). CO₂ decomposition in a packed DBD plasma reactor: influence of packing materials. [10.1039/C5RA27085E]. *RSC Adv*. 6

(45), 39492-39499.

- Rico, V. c. J., Hueso, J. L., Cotrino, J. and González-Elipe, A. n. R. (2010a). Evaluation of Different Dielectric Barrier Discharge Plasma Configurations As an Alternative Technology for Green C1 Chemistry in the Carbon Dioxide Reforming of Methane and the Direct Decomposition of Methanol†. *The Journal of Physical Chemistry A*. 114 (11), 4009-4016.
- Rico, V. J., Hueso, J. L., Cotrino, J. and Gonzalez-Elipe, A. R. (2010b). Evaluation of different dielectric barrier discharge plasma configurations as an alternative technology for green C₁ chemistry in the carbon dioxide reforming of methane and the direct decomposition of methanol. *J Phys Chem A*. 114 (11), 4009-4016.
- Sabine, P., Bert, V., Xin, T., Christophe De, B., Tom, M., Dragana, P., Annemie, B. and Bert, S. (2010). Conversion of carbon dioxide to value-added chemicals in atmospheric pressure dielectric barrier discharges. *Plasma Sources Science and Technology*. 19 (3), 034015.
- Sanjabi, S. and Obeydavi, A. (2015). Synthesis and characterization of nanocrystalline MgAl₂O₄ spinel via modified sol-gel method. *Journal of Alloys and Compounds*. 645, 535-540.
- Seigo, K., Ryo, M., Takumi, Y., Lukman Adi, P. and Tomohiro, N. (2018). Interfacial reactions between DBD and porous catalyst in dry methane reforming. *Journal of Physics D: Applied Physics*.
- Seo, H. (2018). Recent scientific progress on developing supported Ni catalysts for dry (CO₂) reforming of methane. *Catalysts*. 8 (3), 110.
- Seyed Matin, N., Savadkoobi, H. A. and Feizabadi, S. Y. (2008). Methane Conversion to C₂ Hydrocarbons Using Dielectric-barrier Discharge Reactor: Effects of System Variables. [journal article]. *Plasma Chemistry and Plasma Processing*. 28 (2), 189-202.
- Shannon, R. D. and Rossman, G. R. (1991). Dielectric constant of MgAl₂O₄ spinel and the oxide additivity rule. *Journal of Physics and Chemistry of Solids*. 52 (9), 1055-1059.
- Shapoval, V. and Marotta, E. (2015). Investigation on Plasma-Driven Methane Dry Reforming in a Self-Triggered Spark Reactor. *Plasma Processes and Polymers*. 12 (8), 808-816.
- Sheng, Z., Kameshima, S., Sakata, K. and Nozaki, T. (2018). Plasma-enabled dry

- methane reforming *Plasma Chemistry and Gas Conversion*: IntechOpen.
- Shi, X. H., Ban, J. J., Zhang, L., Sun, Z. P., Jia, D. Z. and Xu, G. C. (2017). Preparation and exceptional adsorption performance of porous MgO derived from a metal-organic framework. [10.1039/C7RA00526A]. *RSC Advances*. 7 (26), 16189-16195.
- Sierra Gallego, G. n., Batiot-Dupeyrat, C., Barrault, J. l. and Mondragón, F. (2008). Dual active-site mechanism for dry methane reforming over Ni/La₂O₃ produced from LaNiO₃ perovskite. *Industrial & Engineering Chemistry Research*. 47 (23), 9272-9278.
- Snoeckx, R., Aerts, R., Tu, X. and Bogaerts, A. (2013a). Plasma-Based Dry Reforming: A Computational Study Ranging from the Nanoseconds to Seconds Time Scale. *The Journal of Physical Chemistry C*. 117 (10), 4957-4970.
- Snoeckx, R., Aerts, R., Tu, X. and Bogaerts, A. (2013b). Plasma-based dry reforming: A computational study ranging from the nanoseconds to seconds time scale. *Journal of Physical Chemistry C*. 117 (10), 4957-4970.
- Snoeckx, R. and Bogaerts, A. (2017). Plasma technology -A novel solution for CO₂ conversion? [10.1039/C6CS00066E]. *Chem Soc Rev*. 46 (19), 5805-5863.
- Snoeckx, R., Heijkers, S., Van Wesenbeeck, K., Lenaerts, S. and Bogaerts, A. (2016a). CO₂ conversion in a dielectric barrier discharge plasma: N₂ in the mix as a helping hand or problematic impurity? [10.1039/C5EE03304G]. *Energy & Environmental Science*. 9 (3), 999-1011.
- Snoeckx, R., Heijkers, S., Van Wesenbeeck, K., Lenaerts, S. and Bogaerts, A. (2016b). CO₂ conversion in a dielectric barrier discharge plasma: N₂ in the mix as a helping hand or problematic impurity? *Energy & Environmental Science*.
- Snoeckx, R., Wang, W., Zhang, X., Cha, M. S. and Bogaerts, A. (2018). Plasma-based multi-reforming for Gas-To-Liquid: tuning the plasma chemistry towards methanol. *Sci Rep*. 8 (1), 15929.
- Snoeckx, R., Zeng, Y., Tu, X. and Bogaerts, A. (2015a). Plasma-based dry reforming: can we improve the dielectric barrier discharge process? Proceedings of the 2015a 22nd International Conference on Plasma Chemistry Antwerp, Belgium, 1-12.
- Snoeckx, R., Zeng, Y., Tu, X. and Bogaerts, A. (2015b). Plasma-based dry

- reforming: improving the conversion and energy efficiency in a dielectric barrier discharge. *RSC Advances*. 5 (38), 29799-29808.
- Snoeckx, R., Zeng, Y. X., Tu, X. and Bogaerts, A. (2015c). Plasma-based dry reforming: improving the conversion and energy efficiency in a dielectric barrier discharge. *RSC Adv*. 5 (38), 29799-29808.
- Sohbatzadeh, F. and Soltani, H. (2018). Time-dependent one-dimensional simulation of atmospheric dielectric barrier discharge in N₂/O₂/H₂O using COMSOL Multiphysics. *Journal of Theoretical and Applied Physics*. 12 (1), 53-63.
- Son, I. H., Kwon, S., Park, J. H. and Lee, S. J. (2016). High coke-resistance MgAl₂O₄ islands decorated catalyst with minimizing sintering in carbon dioxide reforming of methane. *Nano Energy*. 19 (Supplement C), 58-67.
- Song, C. (2002). CO₂ Conversion and Utilization: An Overview. 809, 2-30.
- Song, H. K., Choi, J. W., Yue, S. H., Lee, H. and Na, B. K. (2004). Synthesis gas production via dielectric barrier discharge over Ni/γ-Al₂O₃ catalyst. *Catalysis Today*. 89 (1-2), 27-33.
- Song, L., Kong, Y. and Li, X. (2017). Hydrogen production from partial oxidation of methane over dielectric barrier discharge plasma and NiO/γ-Al₂O₃ catalyst. *International Journal of Hydrogen Energy*.
- Spiliopoulos, N., Mataras, D. and Rapakoulias, D. (1997a). Arrhenius-like behavior in plasma reactions. *Applied physics letters*. 71 (5), 605-607.
- Spiliopoulos, N., Mataras, D. and Rapakoulias, D. (1997b). Kinetics of power deposition and silane dissociation in Radio-Frequency discharges. *Journal of The Electrochemical Society*. 144 (2), 634-640.
- Subedi, D. P., Joshi, U. M. and Wong, C. S. (2017). Dielectric barrier discharge (DBD) plasmas and their applications. In R. S. Rawat (Ed.), *Plasma Science and Technology for Emerging Economies: An AAAPT Experience* (pp. 693-737). Singapore: Springer Singapore.
- Tahir, B., Tahir, M. and Amin, N. A. S. (2017). Photo-induced CO₂ reduction by CH₄/H₂O to fuels over Cu-modified g-C₃N₄ nanorods under simulated solar energy. *Applied Surface Science*. 419, 875-885.
- Tahir, B., Tahir, M. and Amin, N. A. S. (2018). Tailoring performance of La-modified TiO₂ nanocatalyst for continuous photocatalytic CO₂ reforming of CH₄ to fuels in the presence of H₂O. *Energy Conversion and Management*. 159, 284-298.

- Tahir, M. and Amin, N. S. (2013). Recycling of carbon dioxide to renewable fuels by photocatalysis: Prospects and challenges. *Renewable & Sustainable Energy Reviews*. 25, 560-579.
- Tahir, M., Tahir, B. and Amin, N. A. S. (2015). Gold-nanoparticle-modified TiO₂ nanowires for plasmon-enhanced photocatalytic CO₂ reduction with H₂ under visible light irradiation. *Applied Surface Science*. 356, 1289-1299.
- Takaki, K., Chang, J.-S. and Kostov, K. G. (2004a). Atmospheric pressure of nitrogen plasmas in a ferroelectric packed bed barrier discharge reactor. Part I. Modeling. *IEEE transactions on dielectrics and electrical insulation*. 11 (3), 481-490.
- Takaki, K., Shimizu, M., Mukaigawa, S. and Fujiwara, T. (2004b). Effect of electrode shape in dielectric barrier discharge plasma reactor for NO_x removal. *IEEE Transactions on Plasma Science*. 32 (1), 32-38.
- Tao, X., Bai, M., Li, X., Long, H., Shang, S., Yin, Y. and Dai, X. (2011). CH₄-CO₂ reforming by plasma – challenges and opportunities. *Progress in Energy and Combustion Science*. 37 (2), 113-124.
- Tao, X., Li, X., Huang, L., Wang, G. and Ye, Q. (2016). Highly active Ni-Ce/TiO₂-Al₂O₃ catalysts: Influence of preparation methods. *International Journal of Hydrogen Energy*. 41 (15), 6271.
- Toth, J. R., Lacks, D. J. and Sankaran, R. M. (2016). Direct conversion of methane by an atmospheric-pressure dielectric barrier discharge microplasma. Proceedings of the 2016 *IEEE International Conference on Plasma Science (ICOPS)*. 19-23 June 2016. 1-1.
- Tu, X., Gallon, H. J., Twigg, M. V., Gorry, P. A. and Whitehead, J. C. (2011a). Dry reforming of methane over a Ni/Al₂O₃ catalyst in a coaxial dielectric barrier discharge reactor. *Journal of Physics D: Applied Physics*. 44 (27), 274007.
- Tu, X., Gallon, H. J., Twigg, M. V., Gorry, P. A. and Whitehead, J. C. (2011b). Dry reforming of methane over a Ni/Al₂O₃ catalyst in a coaxial dielectric barrier discharge reactor. *Journal of Physics D: Applied Physics*. 44 (27), 274007.
- Tu, X. and Whitehead, J. C. (2012). Plasma-catalytic dry reforming of methane in an atmospheric dielectric barrier discharge: Understanding the synergistic effect at low temperature. *Applied Catalysis B: Environmental*. 125, 439-448.
- Tu, X. and Whitehead, J. C. (2014). Plasma dry reforming of methane in an atmospheric pressure AC gliding arc discharge: Co-generation of syngas and

- carbon nanomaterials. *International Journal of Hydrogen Energy*. 39 (18), 9658-9669.
- Usman, M. and Daud, W. M. A. W. (2016). Microemulsion based synthesis of Ni/MgO catalyst for dry reforming of methane. [10.1039/C6RA01652A]. *RSC Advances*. 6 (44), 38277-38289.
- Usman, M., Daud, W. M. A. W. and Abbas, H. F. (2015). Dry reforming of methane: Influence of process parameters-A review. *Renewable & Sustainable Energy Reviews*. 45, 710-744.
- Valentini, A., Carreno, N. L. V., Leite, E. R., Goncalves, R. F., Soledade, L. E. B., Maniette, Y., Longo, E. and Probst, L. F. D. (2004). Improved activity and stability of Ce-promoted Ni/ γ -Al₂O₃ catalysts for carbon dioxide reforming of methane. *Latin American Applied Research*. 34 (3), 165-172.
- Van Laer, K. and Bogaerts, A. (2017). Influence of Gap Size and Dielectric Constant of the Packing Material on the Plasma Behaviour in a Packed Bed DBD Reactor: A Fluid Modelling Study. *Plasma Processes and Polymers*. 14 (4-5), 1600129.
- Vandenbroucke, A. M., Mora, M., Jiménez-Sanchidrián, C., Romero-Salguero, F. J., De Geyter, N., Leys, C. and Morent, R. (2014). TCE abatement with a plasma-catalytic combined system using MnO₂ as catalyst. *Applied Catalysis B: Environmental*. 156-157, 94-100.
- Vandenbroucke, A. M., Morent, R., De Geyter, N. and Leys, C. (2011). Non-thermal plasmas for non-catalytic and catalytic VOC abatement. *J Hazard Mater*. 195, 30-54.
- Wang, H. and Baker, R. T. K. (2004). Decomposition of Methane over a Ni-Cu-MgO Catalyst to Produce Hydrogen and Carbon Nanofibers. *The Journal of Physical Chemistry B*. 108 (52), 20273-20277.
- Wang, J., Wang, Z. and Liu, C.-J. (2014). Enhanced activity for CO oxidation over WO₃ nanolamella supported Pt catalyst. *ACS Applied Materials & Interfaces*. 6 (15), 12860-12867.
- Wang, Q., Cheng, Y. and Jin, Y. (2009a). Dry reforming of methane in an atmospheric pressure plasma fluidized bed with Ni/ γ -Al₂O₃ catalyst. *Catalysis Today*. 148 (3-4), 275-282.
- Wang, Q., Yan, B. H., Jin, Y. and Cheng, Y. (2009b). Investigation of Dry Reforming of Methane in a Dielectric Barrier Discharge Reactor. *Plasma*

Chemistry and Plasma Processing. 29 (3), 217-228.

- Wang, W., Snoeckx, R., Zhang, X., Cha, M. and Bogaerts, A. (2018a). Modeling plasma-based CO₂ and CH₄ conversion in mixtures with N₂, O₂ and H₂O: The bigger plasma chemistry picture. *The Journal of Physical Chemistry C*.
- Wang, Y., Yao, L., Wang, S., Mao, D. and Hu, C. (2018b). Low-temperature catalytic CO₂ dry reforming of methane on Ni-based catalysts: A review. *Fuel Processing Technology*. 169, 199-206.
- Wei, J. M. and Iglesia, E. (2004). Isotopic and kinetic assessment of the mechanism of reactions of CH₄ with CO₂ or H₂O to form synthesis gas and carbon on nickel catalysts. *Journal of Catalysis*. 224 (2), 370-383.
- Wei, Q. H., Gao, X. H., Liu, G. G., Yang, R. Q., Zhang, H. B., Yang, G. H., Yoneyama, Y. and Tsubaki, N. (2018). Facile one-step synthesis of mesoporous Ni-Mg-Al catalyst for syngas production using coupled methane reforming process. *Fuel*. 211, 1-10.
- Whitehead, J. C. (2016). Plasma-catalysis: the known knowns, the known unknowns and the unknown unknowns. *Journal of Physics D-Applied Physics*. 49 (24), 243001.
- Wu, L., Liu, Y., Zhang, L. and Zhao, L. (2014). A green-chemical synthetic route to fabricate a lamellar-structured Co/Co(OH)₂ nanocomposite exhibiting a high removal ability for organic dye. [10.1039/C3DT53369G]. *Dalton Transactions*. 43 (14), 5393-5400.
- Wu, X. D., Shao, G. F., Shen, X. D., Cui, S. and Chen, X. B. (2017). The low temperature fabrication of nanocrystalline MgAl₂O₄ spinel aerogel by a non-alkoxide sol-gel route. *Materials Letters*. 207 (Supplement C), 137-140.
- Xin, T., Helen, J. G., Martyn, V. T., Peter, A. G. and Whitehead, J. C. (2011). Dry reforming of methane over a Ni/Al₂O₃ catalyst in a coaxial dielectric barrier discharge reactor. *Journal of Physics D: Applied Physics*. 44 (27), 274007.
- Xuming, Z. and Min Suk, C. (2013). Electron-induced dry reforming of methane in a temperature-controlled dielectric barrier discharge reactor. *Journal of Physics D: Applied Physics*. 46 (41), 415205.
- Yabe, T., Mitarai, K., Oshima, K., Ogo, S. and Sekine, Y. (2017). Low-temperature dry reforming of methane to produce syngas in an electric field over La-doped Ni/ZrO₂ catalysts. *Fuel Processing Technology*. 158, 96-103.
- Yadav, A. A., Lokhande, V. C., Bulakhe, R. N. and Lokhande, C. D. (2017).

- Amperometric CO₂ gas sensor based on interconnected web-like nanoparticles of La₂O₃ synthesized by ultrasonic spray pyrolysis. [journal article]. *Microchimica Acta*. 184 (10), 3713-3720.
- Yahyavi, S. R., Haghighi, M., Shafiei, S., Abdollahifar, M. and Rahmani, F. (2015). Ultrasound-assisted synthesis and physicochemical characterization of Ni-Co/Al₂O₃-MgO nanocatalysts enhanced by different amounts of MgO used for CH₄/CO₂ reforming. *Energy Conversion and Management*. 97, 273-281.
- Yan, X., Zhao, B., Liu, Y. and Li, Y. (2015). Dielectric barrier discharge plasma for preparation of Ni-based catalysts with enhanced coke resistance: Current status and perspective. *Catalysis Today*. 256, Part 1, 29-40.
- Yang, Y. (2003). Direct non-oxidative methane conversion by non-thermal plasma: Modeling study. [journal article]. *Plasma Chemistry and Plasma Processing*. 23 (2), 327-346.
- Yap, D., Tatibouët, J.-M. and Batiot-Dupeyrat, C. (2015). Carbon dioxide dissociation to carbon monoxide by non-thermal plasma. *Journal of CO₂ Utilization*. 12, 54-61.
- Yap, D., Tatibouët, J.-M. and Batiot-Dupeyrat, C. (2018). Catalyst assisted by non-thermal plasma in dry reforming of methane at low temperature. *Catalysis Today*. 299, 263-271.
- Yu, Q., Kong, M., Liu, T., Fei, J. and Zheng, X. (2012). Characteristics of the Decomposition of CO₂ in a Dielectric Packed-Bed Plasma Reactor. [journal article]. *Plasma Chemistry and Plasma Processing*. 32 (1), 153-163.
- Zeng, Y., Zhu, X., Mei, D., Ashford, B. and Tu, X. (2015). Plasma-catalytic dry reforming of methane over γ -Al₂O₃ supported metal catalysts. *Catalysis Today*. 256, Part 1, 80-87.
- Zeng, Y. X., Wang, L., Wu, C. F., Wang, J. Q., Shen, B. X. and Tu, X. (2017). Low temperature reforming of biogas over K-, Mg- and Ce-promoted Ni/Al₂O₃ catalysts for the production of hydrogen rich syngas: Understanding plasma-catalytic synergy. *Applied Catalysis B: Environmental*.
- Zhang, A.-J., Zhu, A.-M., Guo, J., Xu, Y. and Shi, C. (2010). Conversion of greenhouse gases into syngas via combined effects of discharge activation and catalysis. *Chemical Engineering Journal*. 156 (3), 601-606.
- Zhang, J. G., Wang, H. and Dalai, A. K. (2007). Development of stable bimetallic catalysts for carbon dioxide reforming of methane. *Journal of Catalysis*. 249

(2), 300-310.

- Zhang, K., Mukhriza, T., Liu, X., Greco, P. P. and Chiremba, E. (2015a). A study on CO₂ and CH₄ conversion to synthesis gas and higher hydrocarbons by the combination of catalysts and dielectric-barrier discharges. *Applied Catalysis A: General*. 502, 138-149.
- Zhang, K., Mukhriza, T., Liu, X. T., Greco, P. P. and Chiremba, E. (2015b). A study on CO₂ and CH₄ conversion to synthesis gas and higher hydrocarbons by the combination of catalysts and dielectric-barrier discharges. *Applied Catalysis A-General*. 502, 138-149.
- Zhang, X. L., Lee, C. S. M., Mingos, D. M. P. and Hayward, D. O. (2003). Carbon dioxide reforming of methane with Pt catalysts using microwave dielectric heating. *Catalysis Letters*. 88 (3-4), 129-139.
- Zhang, X. M. and Cha, M. S. (2013). Electron-induced dry reforming of methane in a temperature-controlled dielectric barrier discharge reactor. *Journal of Physics D-Applied Physics*. 46 (41), 415205.
- Zhang, Y.-R., Van Laer, K., Neyts, E. C. and Bogaerts, A. (2016a). Can plasma be formed in catalyst pores? A modeling investigation. *Applied Catalysis B: Environmental*. 185, 56-67.
- Zhang, Y. R., Neyts, E. C. and Bogaerts, A. (2016b). Influence of the Material Dielectric Constant on Plasma Generation inside Catalyst Pores. *Journal of Physical Chemistry C*. 120 (45), 25923-25934.
- Zhang, Z. and Verykios, X. (1994). Carbon dioxide reforming of methane to synthesis gas over supported Ni catalysts. *Catalysis Today*. 21 (2-3), 589-595.
- Zhao, B., Yan, X., Zhou, Y. and Liu, C.-j. (2013). Effect of catalyst structure on growth and reactivity of carbon nanofibers over Ni/MgAl₂O₄. *Industrial & Engineering Chemistry Research*. 52 (24), 8182-8188.
- Zheng, X., Tan, S., Dong, L., Li, S. and Chen, H. (2015a). Plasma-assisted catalytic dry reforming of methane: Highly catalytic performance of nickel ferrite nanoparticles embedded in silica. *Journal of Power Sources*. 274, 286-294.
- Zheng, X. G., Tan, S. Y., Dong, L. C., Li, S. B. and Chen, H. M. (2014). LaNiO₃@SiO₂ core-shell nano-particles for the dry reforming of CH₄ in the dielectric barrier discharge plasma. *International Journal of Hydrogen Energy*. 39 (22), 11360-11367.
- Zheng, X. G., Tan, S. Y., Dong, L. C., Li, S. B. and Chen, H. M. (2015b). Silica-

- coated LaNiO₃ nanoparticles for non-thermal plasma assisted dry reforming of methane: Experimental and kinetic studies. *Chemical Engineering Journal*. 265, 147-156.
- Zheng, X. G., Tan, S. Y., Dong, L. C., Li, S. B., Chen, H. M. and Wei, S. A. (2015c). Experimental and kinetic investigation of the plasma catalytic dry reforming of methane over perovskite LaNiO₃ nanoparticles. *Fuel Processing Technology*. 137, 250-258.
- Zhou, L. M., Xue, B., Kogelschatz, U. and Eliasson, B. (1998). Nonequilibrium plasma reforming of greenhouse gases to synthesis gas. *Energy & Fuels*. 12 (6), 1191-1199.
- Zhu, B., Li, X. S., Liu, J. L., Zhu, X. B. and Zhu, A. M. (2015). Kinetics study on carbon dioxide reforming of methane in kilohertz spark-discharge plasma. *Chemical Engineering Journal*. 264, 445-452.
- Zhu, F., Zhang, H., Yan, X., Yan, J., Ni, M., Li, X. and Tu, X. (2017). Plasma-catalytic reforming of CO₂-rich biogas over Ni/ γ -Al₂O₃ catalysts in a rotating gliding arc reactor. *Fuel*. 199, 430-437.
- Zhu, X. L., Cheng, D. G. and Kuai, P. Y. (2008a). Catalytic decomposition of methane over Ni/Al₂O₃ catalysts: Effect of plasma treatment on carbon formation. *Energy & Fuels*. 22 (3), 1480-1484.
- Zhu, X. L., Huo, P. P., Zhang, Y. P., Cheng, D. G. and Liu, C. J. (2008b). Structure and reactivity of plasma treated Ni/Al₂O₃ catalyst for CO₂ reforming of methane. *Applied Catalysis B-Environmental*. 81 (1-2), 132-140.
- Zouaghi, A., Zouzou, N., Mekhaldi, A. and Gouri, R. (2016). Submicron particles trajectory and collection efficiency in a miniature planar DBD-ESP: Theoretical model and experimental validation. *Journal of Electrostatics*. 82, 38-47.